V. longisporum elicits media-dependent secretome responses with a further capacity to distinguish between plant-related environments

Miriam Leonard[1], Anika Kühn[1], Rebekka Harting[1], Isabel Maurus[1], Alexandra Nagel[1], Jessica Starke[1], Harald Kusch[1], Oliver Valerius[1], Kirstin Feussner[2], Ivo Feussner[2], Alexander Kaever[3], Manuel Landesfeind[3], Burkhard Morgenstern[3], Dörte Becher[4], Michael Hecker[4], Susanna A. Braus-Stromeyer[1], James W. Kronstad[5], Gerhard H. Braus[1*]

1) Department of Molecular Microbiology and Genetics, Institute of Microbiology and Genetics and Goettingen Center for Molecular Biosciences (GZMB), University of Goettingen, Goettingen, Germany.
2) Department for Plant Biochemistry, Albrecht-von-Haller-Institute for Plant Sciences and Goettingen Center for Molecular Biosciences (GZMB), University of Goettingen, Goettingen, Germany.
3) Department of Bioinformatics, Institute of Microbiology and Genetics and Goettingen Center for Molecular Biosciences (GZMB), University of Goettingen, Goettingen, Germany.
4) Department of Microbial Physiology, Institute for Microbiology, Ernst-Moritz-Arndt-Universität Greifswald, Greifswald, Germany.
5) Michael Smith Laboratories, Department of Microbiology and Immunology, University of British Columbia, Vancouver, Canada.

*Corresponding author: Gerhard H. Braus (e-mail: gbraus@gwdg.de)

Abstract

Verticillia cause a vascular wilt disease affecting a broad range of economically valuable crops. The fungus enters its host plants through the roots and colonizes the vascular system. It requires extracellular proteins for a successful plant colonization. The exoproteome of the allodiploid *Verticillium longisporum* was analyzed upon cultivation in different media. Secreted fungal proteins were identified by label free LC-MS/MS screening. *V. longisporum* induced two main secretion patterns. One response pattern was elicited in various non-plant related environments. The second pattern includes the exoprotein responses to the plant-related media, pectin-rich simulated xylem medium and pure xylem sap, which exhibited similar but additional distinct features. These exoproteomes include a shared core set of 223 secreted and similarly enriched fungal proteins. The pectin-rich medium significantly induced the secretion of 144 proteins including a number of pectin degrading enzymes, whereas xylem sap triggered a smaller but unique fungal exoproteome pattern with 32 enriched proteins. The latter pattern included proteins with domains of known effectors, metallopeptidases and carbohydrate-active enzymes. The most abundant and uniquely enriched proteins of these different groups are the necrosis and ethylene inducing-like proteins Nlp2 and Nlp3, the cerato-platanin proteins Cp1 and Cp2, the metallopeptidases Mep1 and Mep2 and the CAZys Gla1, Amy1 and Cbd1. Deletion of the majority of the corresponding genes caused no phenotypic changes during *ex planta* growth or invasion and colonization of tomato plants. However, we discovered that the *NLP2* and *NLP3* deletion strains were compromised in plant infections. Overall, our exoproteome approach revealed that the fungus induces specific secretion responses in different environments. The fungus has a general response to non-plant related media whereas it is able to fine-tune its exoproteome in the presence of plant

material. Importantly, the xylem sap-specific exoproteome pinpointed Nlp2 and Nlp3 as single effectors required for successful *V. dahliae* colonization.

Author Summary

Verticillium spp. infect hundreds of different plants world-wide leading to enormous economic losses. Verticillium wilt is a disease of the vasculature. The fungus colonizes the xylem of its host plant where it exploits the vascular system to colonize the whole plant. Therefore, the fungus spends part of its lifetime in this nutrient-low and imbalanced environment where it is inaccessible for disease control treatments. This lifestyle as well requires the fungus to react to plant defense responses by secreting specific effector molecules to establish a successful infection. We addressed the differences in media-dependent secretion responses of *Verticillium longisporum*. We identified a broad response pattern induced by several media, and a similar response (but with some distinct differences) for the plant-related environments: the pectin-rich medium SXM and xylem sap from the host rapeseed. Importantly, we show that the necrosis and ethylene inducing-like proteins Nlp2 and Nlp3 are xylem sap-specific proteins that are required for full *V. dahliae* pathogenicity on tomato. These factors play a role during the colonization phase and represent potential targets for new control strategies for Verticillium wilt.

Introduction

Vascular wilts caused by *Verticillium* spp. are widespread and destructive plant diseases, resulting in enormous economic losses. Haploid *Verticillium dahliae*, the economically most important representative of the genus, infects over 200 plant species worldwide [1, 2]. In contrast, the allodiploid *Verticillium longisporum* has a narrow host range that comprises primarily *Brassicaceae*. During the last several decades, increasing cultivation of the oilseed rape *Brassica napus* revealed *V. longisporum* as one of the most devastating pathogens of oilseed rape [3].

Verticillium spp. enter the plant through the root, where the fungus then grows both inter- and intracellular in the root cortex towards the central cylinder and finally colonizes the xylem vessels [4, 5]. The transpiration stream plays an essential role in supplying water and mineral salts to the aerial tissue of plants [6]. The xylem sap is a nutrient-poor environment with plant defense proteins, hormones and low concentrations of amino acids and sugars [7, 8]. This makes it a very unique environment, which *Verticillium* spp. exploit for growth and systematic distribution in the host plant [7, 9]. Factors that contribute to adaptation to the unbalanced amino acid supply include the chorismate synthase encoding gene *VlARO2* and the cross-pathway transcription factor *CPC1* [7, 10]. The pathogen requires distinct sets of enzymes during different steps in plant colonization including carbohydrate active enzymes (CAZys) and peptidases, as well as small secreted proteins, to establish an infection and overcome the immune response of the plant. Several extracellular proteins including polygalacturonases, pectate lyases, xylanases or lipases presumably contribute to virulence during pathogen-host interactions [11–15].

The plant immune response depends in part on transmembrane receptor proteins termed pattern recognition receptors (PRRs). Cell surface localized PRRs recognize conserved microbial molecules and structural motifs designated as pathogen-

associated molecular patterns (PAMPs); examples include the fungal cell-wall polymer chitin [16]. PAMP perception elicits a basal defense response which halts colonization by non-adapted pathogens and results in PAMP-triggered immunity (PTI). Host-adapted pathogens circumvent PTI by secretion of specific effector proteins as virulence factors for different phases of the infection cycle [17]. These secreted effectors may act passively or actively to combat plant defense responses [18].

Well known examples of fungal effectors include the Avr4 and Ecp6 effectors from the leaf mold fungus *Cladosporum fulvum* that bind to chitin oligosaccharides via a carbohydrate-binding module (CBM) or LysM domain, respectively [18–21]. Similarly, a chitin scavenging function has also been assigned to Cp1 in *V. dahliae* strain XH-8. *CP1* knockout mutants were affected in cotton virulence [22]. This chitin protection leads to the suppression of the PTI of the plant and shields the fungal cell wall from plant chitinases that hydrolyze chitin [18–21]. Other fungal effectors such as metalloproteases possess enzymatic activity and are able to truncate plant chitinases that attack the fungal cell wall [23, 24]. Toxins provide another means for pathogens to attack plant hosts. For example, necrosis and ethylene inducing-like proteins (NLP) induce immune responses and cell death in host tissues and are conserved among fungi including *Verticillium* spp. [25, 26]. *V. dahliae* isolates encode up to eight NLP homologs [26, 27] whereas most other fungi generally only possess up to three NLPs [25]. Only Nlp1 and Nlp2 show cytotoxic activity in *Nicotiana benthamiana* leaves and play strain- and host-specific roles in *V. dahliae* virulence [26, 27]. Nlp1 and Nlp2 are required for *V. dahliae* JR2 pathogenicity on tomato and *A. thaliana* [26] whereas the corresponding proteins in *V. dahliae* V592 did not alter virulence on cotton [27]. Plant pathogens additionally require a set of carbohydrate-active enzymes (CAZys) that facilitate the breakdown of the plant cell wall [28]. The genomes of *Verticillium* species encode a greater number of cell wall-degrading enzymes with a strikingly high

repertoire of pectin-degrading enzymes compared to the secreted proteins of other plant pathogens [18, 29].

As the fungus lives in the vascular tissues during most of its life cycle in the plant, further knowledge about specific secretion responses would enable a better understanding of fungal-plant interactions during the infection process. Once the fungus resides inside the plant, it is inaccessible for pesticides and therefore the management of Verticillium wilt is very challenging. The most effective and widely used soil fumigants, methyl bromide or metam sodium, are used for high valuable crops, but are not profitable for all crops. Furthermore, these and other banned fungicides, are associated with environmental issues [1, 30]. Therefore, an indispensable approach for protection is to use resistant plant varieties, but these are not available in most crops. The selection pressure on fungal strains to quickly overcome genetic resistances of the plant makes it even more difficult to develop new resistant varieties [1, 18]. Consequently, an increased understanding of the infection process for *Verticillium* spp. is necessary to identify new approaches for disease control.

Until now, it is not known how the effector repertoire of *Verticillium* spp. is expressed once the pathogen enters the plant. Analysis of *Verticillium* strains in their vascular environment is technically demanding, and a large number of plants are required to harvest sufficient amounts of xylem sap. Proteomic approaches can be fruitful because comparison of the intracellular fungal proteome in diluted xylem sap and pectin-rich medium resulted in the identification of a disease-related catalase peroxidase, which was only up-regulated in the presence of xylem sap and not in the presence of pectin [31].

In this study, we extended the comparative analysis with rapeseed xylem sap and focused on the fungal secretome. *V. longisporum* secreted proteins that were derived from cultivation in different growth media were identified by a proteomic approach and

147 the protein patterns induced by different environments were compared. Our goal was
148 to obtain a more comprehensive overview of the secreted factors of *V. longisporum* in
149 response to different substances in its environment that putatively reflect different
150 stages of the infection. We analyzed the exoproteomes of *V. longisporum* on a broad
151 range of media from water to minimal and complete media. As an additional condition,
152 we applied simulated xylem medium (SXM), which is rich in pectin and which was
153 originally developed to mimic the natural plant growth environment, the xylem sap [32].
154 All exoproteomes were compared to fungal cultures grown in extracted xylem sap of
155 the *V. longisporum* host oilseed rape *B. napus*.
156 Our results demonstrate that *V. longisporum* is able to distinguish between the different
157 environments to express different secretome patterns. The pectin-rich medium and
158 xylem sap each triggered distinct protein patterns in comparison to all other tested
159 media. The fungal response to growth in the pectin-rich medium and xylem sap
160 consists of a shared core exoproteome and an additional group of uniquely secreted
161 proteins. A small number of proteins are specifically expressed in xylem sap including
162 CAZys and other potential virulence factors. Of the factors that were specifically
163 enriched in xylem sap, the NLPs, Nlp2 and Nlp3 proteins, we demonstrate
164 contributions to plant pathogenicity as virulence factors.

Results

Xylem sap and pectin-rich SXM trigger specific exoproteomic patterns compared to other growth media

V. longisporum is a rapeseed pathogenic fungus that is able to grow on a variety of different substrates and colonizes the xylem vessels of plants. This requires the adaptation of the fungus to changing nutrient conditions and other biotic and abiotic factors. We examined how different growth media affected the exoproteome of *V. longisporum* with a specific focus on identification of distinct patterns triggered by different plant-related contents. For all experiments, *V. longisporum* was precultured in liquid potato dextrose medium (PDM) to ensure an equal initial growth state prior to the media-specific induction of secretion. The proteins of the *V. longisporum* culture supernatants from different media were precipitated and separated by one-dimensional SDS-PAGE thereby resulting in several different patterns in colloidal Coomassie stained gels (Fig 1A). The defined media conditions corresponded to different levels of complexity including nutrient-free water, water with glucose as carbon source, and a more complex nitrogen-rich medium (YNB: Yeast Nitrogen Base). Several plant-related media were included because the natural habitat of the pathogen *V. longisporum* is inside host plants. These media included the nutrient-limited sucrose medium CDM (Czapek-Dox medium), which was either supplemented with 7% of *B. napus* xylem sap or plant proteins, vegetable juice (V8 juice) and the pectin-rich SXM, which was developed to mimic fungal growth conditions in plants *in vitro* [32, 33]. Finally, we also used extracted xylem sap from the rapeseed plant *B. napus*, corresponding to the natural habitat of the fungus.

To obtain a more comprehensive analysis, complete lanes of the gels with the respective exoproteomes were fractionally subjected to tryptic protein digestion and the resulting peptides were analyzed by LC MS/MS. The obtained raw data were

channeled through a bioinformatics pipeline based on Proteome Discoverer Software 1.3™ (Thermo Scientific) and an in-house genome-wide protein sequence database of *V. longisporum*. The received spectral counts were compared on single secreted protein level by color-coded one-dimensional self-organizing maps (Fig 1B). These revealed that proteins that were strongly enriched in xylem sap or SXM were not enriched in any other condition. Differences in the exoproteome signatures are also illustrated by sample clustering in a principle component analysis plot (Fig 1C). Exoproteomes of *V. longisporum* derived from very diverse media including nutrient-free water, V8 juice, CDM or YNB medium show a similar pattern. Supplementation of CDM with *B. napus* plant proteins or xylem sap with a final concentration of 7% did not result in a different exoproteome pattern, neither did glucose supplementation to water. Therefore, the respective results for these conditions were combined together. In contrast, proteins secreted in pectin-rich SXM or xylem sap each showed a distinct pattern in comparison to the other media conditions. These patterns representing the latter exoproteomes are similar in some features as the clusters lie close to each other on the x-axis, although some differences are present as analyzed further below.

Overall, our analysis illustrates that the fungus has the potential to form a general secretome response to non-plant related environments and, in addition, a similar, but more specialized response to plant-related substances (Fig 1C).

Pectin-rich medium and xylem sap elicit distinct *V. longisporum* exoproteome responses

Similarities and differences of the specific *V. longisporum* exoproteome responses in the pectin-rich SXM compared to xylem sap were analyzed in more detail in a large-scale experimental set up. The protein patterns of six biological replicates of each

cultivation condition were compared. The proteins were precipitated from the culture supernatants, subjected to LC MS/MS and analyzed. The data set was filtered with a statistical workflow using MarVis-Suite [34]. S1 Table shows the identities of the 445 proteins from an in-house database with their protein sequences and details on their abundance as measured by identified peptides. The list is sorted according to the most specifically enriched proteins in xylem sap (green) and SXM (red), respectively. Proteins that are not considered as specifically enriched are listed at the bottom of the table and belong to the core exoproteome.

Clustering analysis of spectral count data of the 445 proteins with MarVis-Suite was visualized as a one-dimensional self-organizing map (Fig 2A). Upper and lower rows represent the two growth conditions, SXM and xylem sap, and each column corresponds to one identified protein. The spectral counts were normalized and color-coded according to the indicated scale where red columns indicate increased and dark blue columns no spectral counts. A set of proteins, which have a stable abundance in both conditions is considered as the shared core exoproteome. Proteins that showed different peptide counts in the two growth conditions were considered as differentially enriched (Fig 2A, ‘enriched in Xylem sap’ and ‘enriched in SXM’, respectively).

V. longisporum is an allodiploid organism derived from two parental strains, and *V. longisporum* 43 used in this study is a result of an A1xD1 hybridization event. A1 and D1 are described as so far unknown haploid *Verticillium* species, of which D1 is closely related to *V. dahliae* and A1 is distantly related to *V. alfalfae* [2]. Most genes are encoded in two copies, reflecting the two isogenes of both parental lineages. BLAST searches against the *V. dahliae* JR2 and the *V. alfalfae* VaMs.102 proteomes from Ensembl Fungi [35] were conducted. As a consequence, two isogene products were detected for most identified proteins.

242 The list of proteins was further and thoroughly analyzed manually to functionally
243 classify the candidates. As the Ensembl Fungi annotations are more robust, further
244 analyses are based on the *V. dahliae* JR2 protein sequences except for candidates
245 with no corresponding hit in *V. dahliae*. Here, the protein sequences for further
246 analyses were retrieved from the *V. alfalfae* VaMs.102 proteome [35]. Putative
247 functions of robust annotated proteins were addressed with InterProScan [36], the
248 CAZy database (http://www.cazy.org) and dbCAN2 [37]. All details are given in S2
249 Table. The Venn diagram in Fig 2B displays the 399 candidates with robust
250 annotations in different groups. Protein extracts from pectin-rich SXM and xylem sap
251 share a core exoproteome of 223 proteins with a similar abundance in both media, but
252 each also induced the secretion of distinct exoprotein patterns. SXM cultivation
253 resulted with 144 secreted proteins in a four-fold higher number of secreted proteins
254 specifically enriched in comparison to xylem sap, where the peptide count of 32
255 proteins was specifically increased (Fig 2B).
256 These results show that SXM, which is used to simulate xylem sap *in vitro,* and xylem
257 sap of *B. napus* induce distinct secretion responses with different facets. This indicates
258 that the fungus is able to fine-tune its secretion responses.
259
260 **_V. longisporum_ secretes a broad arsenal of substrate-degrading enzymes in**
261 **pectin-rich medium and in xylem sap**
262 All 399 identified secreted proteins were classified into functional groups according to
263 the predicted domains (S2 Table, Fig 2C). For 65 identified proteins, classified as
264 hypothetical gene products, no information about structural domains or putative
265 functions could be found ('Unknown'). 'Proteins involved in lipid metabolism', 'Effectors'
266 and smaller groups combined as 'Others' represent minor groups. More proteins were
267 sorted to 'Proteins involved in redox processes' (9%) or 'Peptidases' (16%) whereas

the functional classification revealed an overrepresentation of proteins involved in carbohydrate metabolism or catabolism with around 40% of proteins acting on carbohydrates and another 5% of proteins with domains interacting with carbohydrates (Fig 2C, S3 Table).

Further analysis of proteins from functional groups regarding the induction by different media showed that pectin-rich medium predominantly triggered the secretion of carbohydrate-degrading enzymes, but also peptidases and redox enzymes (Fig 2D, S3 Table). No effectors were found in the SXM-specific exoproteome. Cultivation in xylem sap triggered the unique secretion of carbohydrate-degrading enzymes, effectors, peptidases and redox enzymes though the total number of enriched proteins is significantly smaller compared to the SXM-specific secreted proteins.

The majority of identified secreted proteins comprise the carbohydrate-active enzymes, which contain protein motifs that have been classified into sequence-related families of CAZy modules [38]. Within the group of all secreted proteins we identified 96 glycoside hydrolases (GHs), 36 polysaccharide lyases (PLs), 21 carbohydrate esterases (CEs), one glycosyltransferase (GT), 19 auxiliary activities (AAs). Of these CAZys, 21 proteins additionally possess non-catalytic, carbohydrate-binding modules (CBMs) (Fig 2E, S4 Table). In the proteins from the pectin-rich medium condition, the CAZys are highly represented with 64 proteins whereas in xylem sap only 19 CAZys are specifically enriched and 90 proteins belong to the core exoproteome (S4 Table). The core exoproteome exhibits an overrepresentation of CAZy families with 32 proteins acting on pectin, including members of family GH28 (five proteins), PL1 (16 proteins), PL3 (seven proteins) and CE8 (four proteins). Additionally, the SXM-specific and most enriched CAZy families comprise 20 pectin-degrading enzymes (families GH28, PL1 and CE12 with ten, six and four proteins, respectively, S4 Table). Only a

293 few CAZys were specifically enriched in the xylem sap condition, and these were
294 distributed in different families.
295 Overall, we found that *B. napus* xylem sap and pectin-rich SXM, employed as plant-
296 related culture environments, predominantly induced the secretion of carbohydrate-
297 degrading enzymes. Compared to the rapeseed xylem sap condition, SXM triggered
298 an additional set of CAZys that were specifically enriched after cultivation in this
299 medium.
300
301 **Xylem sap triggers the secretion of potential and known *Verticillium* effectors**
302 Compared to the pectin-rich SXM, *V. longisporum* formed a more specific secretion
303 response in xylem sap with only 32 proteins that are uniquely enriched. This indicates
304 that the fungus can distinguish between xylem sap and the presence of other plant
305 material and accordingly fine-tunes its protein secretion. Furthermore, the proteins
306 secreted in the host xylem sap might be specifically important during plant colonization.
307 Table 1 displays the xylem sap-specific proteins. The corresponding isogenes are
308 paired up and the best hit in *V. dahliae* JR2 is given, except for the *V. alfalfae* specific
309 proteins that were searched against the *V. alfalfae* VaMs.102 proteome (Ensembl
310 Fungi). Within the identified groups, proteins were ranked according to the quotient of
311 peptide counts identified in xylem sap (XyS) by the number detected in the pectin-rich
312 SXM. Displayed peptide counts were averaged from 6 biological replicates. If the
313 number was below 1, it was calculated as 0 and the quotient was given as the average
314 XyS peptide counts (>). The 32 xylem sap-specific proteins comprise 15 ‘Proteins
315 acting on carbohydrates’, five ‘Proteins with domains interacting with carbohydrates’,
316 five ‘Effectors’, four ‘Peptidases’, two ‘Proteins involved in redox processes’ and one
317 with a ubiquitin binding domain that was grouped as ‘Other’ (Table 1).

318 Several potential virulence factors were identified in the xylem sap-specific response
319 set. Proteins involved in the degradation of carbohydrates are known to contribute to
320 *V. dahliae* pathogenicity [39, 40]. The five proteins comprising domains of already
321 characterized *V. dahliae* effectors incorporate either necrosis-inducing protein (NPP1,
322 also necrosis-inducing *Phytophthora* protein) or cerato-platanin (CP) domains. NPP1
323 domains are characteristic for necrosis and ethylene inducing-like proteins (NLP) of
324 which *Verticillium* spp. contain up to eight members [26]. Nlp1 and Nlp2 were
325 previously shown to differentially contribute to *V. dahliae* pathogenicity on different
326 hosts [26, 27, 41]. Our secretome approach identified four isogene products
327 corresponding to two NLPs, Nlp2 and Nlp3. Of the CP domain-containing proteins, one
328 isogene assigned to Cp2 was identified as specifically enriched in xylem sap.
329 *V. dahliae* possesses two CP proteins of which Cp1 affects virulence on cotton [22].
330 Additionally, four isogenes of two metallopeptidases were found in the xylem sap-
331 specific secretome. Metalloproteases are able to truncate host defense proteins such
332 as chitinases and therefore have the potential to act as virulence factors [23].
333 These findings show that *V. longisporum* finetunes its protein secretion response in
334 the host xylem sap, which include known and potential effectors important for plant
335 colonization or infection.

Table 1. Xylem sap-specific exoproteins of *V. longisporum*.

	Name	Vl43 identifier	Best Hit *V. dahliae* JR2	Protein domain	Peptide counts		XyS/ SXM	s/l ratio
					SXM	XyS		
Proteins acting on carbohydrates	**Gla1**	vl43-au16.g17458.t1	VDAG_JR2_Chr8g11020a	Glycoside hydrolase 15, Carbohydrate binding module family 20	0	8.2	**>8.2**	0.76
		vl43-au16.g13024.t1			0	3.8	**>3.8**	0.62
	Amy1	vl43-au16.g6892.t1	VDAG_JR2_Chr7g03330a	Glycoside hydrolase 13	1.5	12	**8**	0.68
		vl43-au16.g9360.t1	*V. alfalfae*: VDBG_05827	Glycosyl hydrolases 134	0	7.5	**>7.5**	0.77
		vl43-au16.g6746.t1	VDAG_JR2_Chr3g11080a	Glycoside hydrolase 43	1.2	7.8	**6.5**	0.68
		vl43-au16.g12522.t1			1	5.8	**5.8**	0.61
		vl43-au16.g12596.t1	VDAG_JR2_Chr6g04040a	Glycosyl hydrolases 11	0.8	5.2	**>5.2**	0.55
		vl43-au16.g15027.t1	VDAG_JR2_Chr6g09340a	Polysaccharide lyase 6	2.2	11.2	**5.1**	0.57
		vl43-au16.g5309.t1			2.3	10.8	**4.7**	0.59
		vl43-au16.g207.t1	VDAG_JR2_Chr1g06940a	Glycoside hydrolase 16	2.2	9	**4.1**	0.56
		vl43-au16.g14986.t1			2.3	9.5	**4.1**	0.55
		vl43-au16.g15947.t1	VDAG_JR2_Chr3g00250a	Glycoside hydrolase 131	1	4	**4**	0.43
		vl43-au16.g9097.t1	*V. alfalfae*: VDBG_03110	Glycoside hydrolase 12	1	2.8	**2.8**	0.38
		vl43-au16.g16765.t1	VDAG_JR2_Chr1g04240a	Glycosyl transferase 1	0.3	1.7	**>1.7**	0.49
		vl43-au16.g9025.t1	VDAG_JR2_Chr7g01210a	Carbohydrate esterase 1, Carbohydrate binding module family 1	0.2	1.3	**>1.3**	0.49
Proteins with domains interacting with carbohydrates	**Cbd1**	vl43-au16.g11636.t1	VDAG_JR2_Chr4g04440a	Auxiliary activity 13, Carbohydrate binding module family 20	1.7	13.8	**8.1**	0.71
		vl43-au16.g3945.t1			1.3	6.8	**5.2**	0.55
		vl43-au16.g5519.t1	VDAG_JR2_Chr6g09790a	Auxiliary activity 9	2	8.2	**4.1**	0.51
		vl43-au16.g20506.t1			2.3	8.8	**3.8**	0.46
		vl43-au16.g11273.t1	VDAG_JR2_Chr6g05220a	WSC Carbohydrate binding domain	3.2	11.7	**3.7**	0.46
Effectors	**Nlp3**	vl43-au16.g9727.t1	VDAG_JR2_Chr4g05950a	Necrosis inducing protein	0.3	8.3	**>8.3**	0.84
		vl43-au16.g96.t1			0.2	6.3	**>6.3**	0.81
	Nlp2	vl43-au16.g3884.t1	VDAG_JR2_Chr2g05460a	Necrosis inducing protein	1	4.8	**4.8**	0.61
		vl43-au16.g12566.t1			1.8	6.5	**3.6**	0.47
	Cp2	vl43-au16.g16459.t1	VDAG_JR2_Chr2g07000a	Cerato-platanin	0.3	1.8	**>1.8**	0.41
Peptidases	**Mep2**	vl43-au16.g19470.t1	VDAG_JR2_Chr1g21900a	Peptidase M43	1	8.8	**8.8**	0.57
		vl43-au16.g11262.t1			1.3	8.7	**6.7**	0.55
	Mep1	vl43-au16.g19320.t1	VDAG_JR2_Chr8g09760a	FTP domain, Peptidase M36, fungalysin	1.7	14	**8.2**	0.69
		vl43-au16.g14388.t1			1.8	13.5	**7.5**	0.65
Proteins involved in redox processes		vl43-au16.g2684.t1	VDAG_JR2_Chr8g10630a	FAD-binding domain	6	13.2	**2.2**	0.33
		vl43-au16.g13340.t1			8	15.3	**1.9**	0.34
Other		vl43-au16.g18734.t1	VDAG_JR2_Chr1g04640a	Ubiquitin 3 binding protein But2, C-terminal	9.7	18.8	**1.9**	0.37

Vl43 = *V. longisporum* 43; SXM = simulated xylem medium; XyS = xylem sap; s/l = signal-to-level; FTP = fungalysin/thermolysin propeptide; WSC = putative carbohydrate-binding domain

Xylem sap-specific secreted proteins are dispensable for *V. dahliae ex planta* development

V. longisporum formed a specific secretion response in xylem sap compared to other media showing that the fungus can distinguish between xylem sap and the presence or absence of other plant material. To investigate whether the xylem sap-specific proteins play a major role in fungal colonization of the plant, the top candidates of the protein groups that have been shown to play critical roles in plant colonization [5, 22, 26] were analyzed in this study.

Chosen proteins are highlighted in Table 1 with a bold given name. The follow up genetic analyses of these proteins were conducted with *V. dahliae* JR2 because it can be more easily manipulated genetically compared with the allodiploid *V. longisporum* strain. All candidates from the group “Effectors” were included in the follow up experiments. These comprise two NLPs, Nlp2 and Nlp3, and the Cp2 protein. The *V. dahliae* JR2 homolog of *CP1* was tested as well. Cp1 is a virulence factor of *V. dahliae* strain XH-8 in infections on cotton [22]. The peptidases that were identified as specifically enriched in xylem sap were named Mep1 and Mep2 and were both included in our genetic analyses. Of the largest group, proteins involved in carbohydrate degradation, the three most highly abundant candidates, the glucoamylase Gla1, the carbohydrate-binding module containing protein Cbd1, and the α-amylase Amy1, were further investigated.

For the construction of the corresponding deletion mutants, the open reading frame (ORF) was replaced with either the nourseothricin or hygromycin resistance cassette under control of the constitutively active *gpdA* promoter and *trpC* terminator. Correct integration of the deletion cassette was verified by Southern hybridization (S1-S4 Figs). To investigate a putative combined effect of proteins in similar groups, the following double deletion strains were constructed as well: *NLP2*/*NLP3*, *MEP1/MEP2* and

CP1/CP2. Ectopic complementation strains were also constructed for the *CP1* and *CP2* deletion mutants. Phenotypical analysis of all strains revealed no alteration compared to *V. dahliae* JR2 wildtype (WT) growth and development on solid agar plates such as minimal and complete medium, and simulated xylem medium. Additionally, the strains were tested for the involvement in stress responses with at least one stressor tested for each strain. The stress inducing agent was added to minimal medium. The cell wall perturbing agents SDS and ethanol or the oxidative stressor hydrogen peroxide were used. All single deletion, double deletion and complementation strains exhibited a similar morphological development to *V. dahliae* WT, which is exemplified by growth on SXM (Fig 3).

Overall, these results suggest that Cp1, Cp2, Nlp2, Nlp3, Mep1, Mep2, Gla1, Cbd1 and Amy1, that were found to be enriched specifically in xylem sap cultures, are dispensable for vegetative growth, development and stress response of *V. dahliae*.

Xylem sap-specific CAZys, metalloproteases and cerato-platanin proteins are dispensable for *V. dahliae* JR2 pathogenicity in tomato infections

The functions of the proteins that were specifically enriched after cultivation in xylem sap would be predicted to be important in the interaction with plant substrates in the host xylem sap. Therefore, all *V. dahliae* single and double deletion strains were tested for their virulence on tomato. Ten-day-old tomato seedlings were root-inoculated with the indicated mutant strains, and plants treated with demineralized water were used as mock controls. Disease symptoms were measured three weeks after inoculation and included the height of the plant, the longest leaf length and the fresh weight of the aerial part of the plant. The stack diagrams display the percentage of plants exhibiting the respective symptoms (Figs 4, 5). We found that plants infected with *GLA1, CBD1, AMY1, MEP1, MEP2, MEP1/MEP2, CP1, CP2, CP1/CP2* deletion strains or *CP1* or

393 *CP2* complementation strains showed similar disease symptoms as the WT-infected
394 plants. That is, all fungal infections resulted in a similar stunting phenotype as WT
395 colonization, and plant defense reactions were observed by the discoloration of the
396 hypocotyls in all infected plants.
397 These experiments demonstrated that the tested CAZys or two genes encoding
398 metalloproteases or cerato-platanin proteins do not affect *V. dahliae* pathogenicity
399 under the tested conditions.
400

401 **Nlp3-GFP is secreted into the extracellular space**

402 As described above, two necrosis and ethylene inducing-like proteins were detected
403 in the xylem sap-specific exoproteome. Members of this group are known to contribute
404 to *V. dahliae* pathogenicity and to exhibit host-specific roles [26, 27, 41]. Nlp1 and Nlp2
405 contribute to *V. dahliae* JR2 virulence on tomato and *Arabidopsis* [26], whereas
406 corresponding proteins in *V. dahliae* V592 did not alter virulence on cotton [27].
407 Additionally, Nlp3 did not show any cytotoxic activity on *N. benthamiana* and has not
408 been further characterized [26]. Because our exoproteome approach identified Nlp2
409 and Nlp3 as specifically secreted in xylem sap, we subsequently carried out additional
410 analyses of the roles of these proteins.
411 To monitor the secretion of Nlp3 in liquid media, the gene was fused with a C-terminal
412 *GFP* tag to *NLP3* under the control of the constitutive strong *gpdA* promoter. *V. dahliae*
413 JR2 and *NLP3* deletion strains ectopically overexpressing *NLP3-GFP* were confirmed
414 by Southern hybridization (S1 Fig). Growth characteristics of the strains expressing
415 *NLP3-GFP* were analyzed as described for the other deletion strains. Similar to the
416 deletion strains, the *NLP3-GFP* overexpressing mutants did not show any significant
417 growth variation in comparison to the WT strain under the tested conditions as shown
418 on CDM plates (S5 Fig). Confocal microscopy of the *NLP3-GFP* strains confirmed the

419 production of a GFP signal derived by the Nlp3-GFP fusion protein with an intracellular
420 location at vacuoles (Fig 6A). The expression and secretion of the fusion protein was
421 analyzed by western experiments using a 24 h-old SXM culture. Intracellular proteins
422 were extracted from fungal mycelium, extracellular proteins were precipitated from the
423 culture supernatant and subjected to SDS-PAGE. Western analysis of the *NLP3-GFP*
424 strain confirmed the overexpression and secretion of the fusion protein in pectin-rich
425 medium (Fig 6B). WT and *NLP3* deletion strains ectopically overexpressing *NLP3-GFP*
426 (WT*/OE-NLP3-GFP* and Δ*NLP3/OE-NLP3-GFP,* respectively) revealed strong signals
427 for Nlp3-GFP with a size of 52 kDa in extracellular extracts after probing with α-GFP
428 antibody whereas intracellular protein extracts result in faint bands at the size of the
429 fusion protein as well as for free GFP (~27 kDa). For the control strain *V. dahliae* JR2
430 expressing free GFP (WT/OE-*GFP*) no signal was detected in extracellular space and
431 a strong GFP signal was detected in intracellular extracts. These data corroborate that
432 Nlp3 is primarily a secreted protein and its expression levels neither influence growth
433 nor development.
434
435 **Necrosis and ethylene inducing-like proteins Nlp2 and Nlp3 contribute to**
436 ***V. dahliae* virulence on tomato**
437 Nlp2 only exhibited minor effects in the *V. dahliae*-tomato system [26] whereas Nlp3
438 has not been tested for *V. dahliae* pathogenicity. We first analyzed the adherence to
439 the root and further root colonization of the *NLP3* deletion strain on *A. thaliana* with
440 fluorescence microscopy. The *NLP3* deletion strain expressing free *GFP* under the
441 control of the *gpdA* promoter (Δ*NLP3/OE-GFP*) and the WT control overexpressing
442 *GFP* (WT*/OE-GFP*) were used for root inoculation of three-week-old *Arabidopsis*
443 seedlings. The root colonization at three and five days post inoculation was
444 indistinguishable between WT*/OE-GFP* and Δ*NLP3/OE-GFP* (Fig 7A). Initial root

colonization was observed at three days following inoculation and whole roots were covered with fungal hyphae after five days suggesting that Nlp3 is dispensable for *A. thaliana* root colonization.

Furthermore, the effect on pathogenicity towards tomato was investigated. Tomato infections were carried out as described above. All tested deletion strains were compromised in virulence compared to WT, but the plants nevertheless developed disease symptoms (Fig 7B). All infected plants exhibited stem discolorations and fungal outgrowth was detected from surface sterilized stems (Fig 7C, bottom row). Symptom development in plants colonized with deletion strains was less severe compared to WT infection. An overview of the trays with 15 treated plants, which is a representative number of plants considering fluctuations in the infection success, nicely demonstrate the differences between different strains (Fig 7C, top row). A representative plant also demonstrated the less stunted phenotype of plants treated with *NLP2* and *NLP3* single and double deletion strains in comparison to WT infected plants (Fig 7C, 2nd row). Translating the disease symptoms into the different categories revealed that about 60% of tested plants exhibited no or only mild symptoms compared to approximately 25% of the WT-treated plants (Fig 7B). Infections with the Δ*NLP2*Δ*NLP3* strain resulted in a similar disease index compared to the single deletion strains and, therefore, showed no additive effect of the two deleted *NLP* genes.

In conclusion, the infection study demonstrated that *NLP2* and *NLP3* contribute to *V. dahliae* JR2 virulence on tomato. Deletion of the genes still resulted in induction of disease symptoms suggesting that the fungal strains are well able to penetrate the plant and that Nlp2 and Nlp3 play primarily a role inside of the plant. This is consistent with the exoproteome approach that identified Nlp2 and Nlp3 as xylem sap-specific secretion proteins, in accordance with a role during later infection steps in the xylem

vessels. These experiments show that our proteomic approach successfully identified a xylem sap-specific group that includes proteins that are uniquely required in the xylem sap of the plant. While other tested proteins may have redundant functions, we were able to identify NLPs, which are only secreted in a specific environment, as candidates important for *Verticillium* infection.

Discussion

Fungi require sensing and adapting mechanisms throughout their life cycle. Different environmental cues induce different secretion responses enabling the pathogen to react to changes in e.g. nutrient supply or host defense responses [42].

Our experiments provide evidence for the ability of the allodiploid *V. longisporum* to distinguish between different environments and to induce media-dependent secretion responses. *V. longisporum* secretes a general protein response pattern in various non plant-related media, which reflects a situation outside of the plant. During cultivation in pectin-rich SXM or plant-extracted xylem sap, the fungus reacts to its surrounding and secretes specific proteins important for the degradation of plant material and the colonization of the xylem. These results imply a complex recognition of plant material in the environment and further show that SXM lacks the full capacity to mimic the natural growth medium xylem sap.

Xylem sap consists of water, plant defense proteins, hormones and low concentrations of amino acids and sugars that are transported to upper parts of the plant through the transpiration stream [7, 8]. SXM was developed to mimic the *in planta* environment, but mainly contains amino acids and the complex carbon source pectin [32]. Pectin is found in plant cell walls where it strengthens the wall integrity [43]. The degradation of this complex branched polysaccharide demands the action of several carbohydrate-active enzymes [39]. This situation is reflected in our SXM-derived exoproteome. In the SXM-specific and the core exoproteome we found 64 and 90 CAZys, respectively, of which the enzymes acting on pectin are especially overrepresented with 32 and 20 proteins. Other studies examined the upregulation of fungal genes after *V. dahliae* root-inoculation of *A. thaliana* seedlings for one day [44]. Of these upregulated genes, we identified corresponding proteins are found in our xylem sap-specific as well as the SXM-specific and core exoproteome. Another study on the *V. dahliae* secretome used

minimal medium with cotton root fragments [22]. Several secreted proteins were identified including 12 cellulases, five pectate lyases, two chitinases, 13 proteases and one cerato-platanin domain containing protein (Cp1) [22]. A number of these proteins were detected in our SXM-specific and core exoproteome. However, no overlap to our xylem sap-specific secretome was detected suggesting that the SXM-induced response of *Verticillium* spp. is more similar to the presence of root fragments. In contrast, the exoproteome after contact with the living plant shows an overlap to our SXM- and xylem sap-derived exoproteomes.

The xylem sap is a unique niche for fungal growth due to its low and imbalanced nutrient supply [7, 8]. It therefore is likely quite important for *Verticillium* to recognize this specific environment and adapt to it by secreting colonization-related proteins. In prior studies, we demonstrated that *V. longisporum* changes its growth according to the presence or absence of host xylem sap [31]. The fungus is able to adapt to the low-nutrient and imbalanced amino acid supply in the xylem sap by activating the cross-pathway [10]. In filamentous fungi, this process is controlled by the cross-pathway control transcription factor Cpc1, which is encoded by a homolog of the yeast gene *GCN4* (general control non-derepressed) [10, 45, 46]. Knockdowns in *V. longisporum* and knockouts in *V. dahliae* revealed that Cpc1 is required for growth under amino acid starvation conditions and successful colonization of the host plants [10]. These findings show that *V. longisporum* senses and reacts to its host environment to survive.

The haploid *V. dahliae* responds differently in a susceptible and tolerant olive cultivar [47]. In the susceptible cultivar, the fungus significantly induced expression of genes involved in niche-adaptation, pathogenicity and microsclerotia development [47]. Similarly, the transcriptome of two *V. dahliae* strains with different virulence levels on

528 cotton were analyzed. The strain with reduced virulence exhibited more repressed
529 genes, of which most are related to pathogenesis [48]. These results corroborate that
530 the fungus senses its environment and responds with different secretion patterns.
531 Another tight and fast adapting control mechanism of gene expression lies in chromatin
532 modifications, which can be induced by environmental changes [49]. Such an
533 epigenetic-mediated control has been observed for effector expression in
534 *Leptosphaeria maculans.* Effector genes often reside in AT-rich regions of the genome.
535 These are associated with heterochromatin and explain the silenced state of effector
536 expression. Upon leaf infection chromatin-mediated repression is abolished and gene
537 expression is upregulated in *L. maculans* [50, 51]. As *V. longisporum* responds to the
538 presence of plant-related compounds by inducing specific exoproteome patterns, it will
539 be interesting to shed light on a putative chromatin modification contribution to these
540 unique responses.
541
542 Transcriptional regulators can induce the gene expression of several effectors at once.
543 For example, the transcription factors Som1, Vta2 and Vta3, that are required for
544 sequential steps of infection, control similar but also distinct sets of secreted proteins
545 involved in virulence [52, 53]. All three proteins are involved in the regulation of, for
546 example, *NLP2* [52, 53]. The expression of the two cytotoxic NLPs, *NLP1* and *NLP2*,
547 from *V. dahliae* has been analyzed during host colonization. When colonizing tomato
548 plants, both transcript levels were elevated although only *NLP1* expression was
549 increased during colonization of tobacco plants. The *in planta* expression of *NLP1* and
550 *NLP2* corresponds to the infection phenotype of the deletion strains [26]. These results
551 confirm the hypothesis of a sensitive control mechanism. It shows that effectors may
552 act host-specifically and are only expressed in suitable hosts supporting the idea of a
553 fine-tuned response.

In this study, we identified two NLPs, Nlp2 and Nlp3, as effectors specifically secreted in xylem sap. Single and double deletions of the corresponding genes resulted in compromised pathogenicity on tomato. The *NLP2* single deletion strain was included as control as it was shown previously to contribute to *V. dahliae* virulence [26]. The *NLP3* deletion strain was additionally tested for *A. thaliana* root colonization revealing no differences to WT (Fig 7A). This indicates that Nlp3 is dispensable for root adhesion or colonization but is required during later steps of the infection. NLPs characteristically induce necrotic lesions [27] thus supporting their activity inside of the plant.

Other xylem sap-specifically enriched candidates did not show an effect on *V. dahliae* pathogenicity on tomato. This may be due to redundant or greater contributions of the hundreds of secreted *Verticillium* effectors [29]. Our approach revealed a high number of CAZys among the *V. longisporum* secretome representing 173 out of the total 399 identified proteins (S4 Table). Overall, the *V. dahliae* genome exhibits a strikingly high repertoire of CAZys, especially pectin-degrading enzymes [29]. This suggests that proteins with redundant functions are secreted and explains the WT-like infections of *V. dahliae* strains lacking one of the tested CAZys (glucoamylase Gla1, putative polysaccharide mono-oxygenase Cbd1 and α-amylase Amy1).

We identified two metalloproteases, Mep1 and Mep2, belonging to two different groups of metalloproteases (M36 and M43, respectively) as xylem sap-specific secreted proteins. Metalloproteases promote fungal virulence by degrading host proteins [54, 55]. Plant chitinases degrade chitin of the fungus, which elicits the plant defense response [56]. *V. dahliae* possesses the ability to truncate extracellular chitin-binding domain-containing chitinases [24, 54]. The *V. dahliae* proteome comprises two M43 and six M36 peptidases implicating that other metallopeptidases are able to complement the absence of Mep1 and Mep2. Furthermore, synergistic actions of

579 metallo- and serine proteases have been reported in *F. oxysporum* [54], providing
580 more evidence for the hypothesis of functional redundancy.
581 We also investigated on the cerato-platanin domain containing proteins Cp1 and Cp2.
582 Cp1 was first identified in the exoproteome of the *V. dahliae* strain XH-8 when
583 incubated in minimal medium supplemented with cotton root fragments. In this system,
584 Cp1 was required for cotton virulence and is suggested to function as a chitin
585 scavenger to prevent fungal recognition by the plant [22]. We detected Cp1 in our core
586 exoproteome and included it in our study to investigate on putative synergistic actions
587 of the two CPs present in the *V. dahliae* genome. Our results show that Cp1 and Cp2
588 are dispensable for *V. dahliae* pathogenicity on tomato. These results indicate that
589 effectors may have strain- and host-specific activities.
590 To our knowledge, our proteomic study is the first report identifying the differences
591 between the secretion responses of *V. longisporum* in host xylem sap, the xylem sap
592 mimic SXM and other media. Non-plant related environments elicited a similar broad
593 exoproteome pattern whereas the plant-related media, SXM and xylem sap, induced
594 similar but also distinct responses. These results indicated that the fungus has the
595 capacity to sense differences in the presence of plant-related compounds and
596 therefore rules out SXM as xylem sap mimic. Additionally, our approach identified
597 necrosis and ethylene inducing-like proteins Nlp2 and Nlp3 in the xylem sap-specific
598 secretome. These proteins are required for *V. dahliae* pathogenicity with roles in later
599 steps of infection and display potential targets for control strategies of Verticillium wilt.

Materials and Methods

Fungal strains and growth conditions

Verticillium strains (S5 Table) were cultivated in liquid simulated xylem medium (SXM) modified from [32] as described in [57] for conidiospore formation and in liquid potato dextrose medium (PDM) (Potato Dextrose broth (Carl Roth)) for mycelial growth. Cultures were incubated at 25°C under constant agitation at 115 – 125 rpm. For long-term storage spores were maintained in closed vials with 25% glycerol at -80°C.

For the exoproteome comparison, *V. longisporum* 43 (Vl43) was inoculated with 1.5 x 10^6 spores per 150 ml PDM (150 rpm) and incubated for four days. Each culture was centrifuged and the mycelium and spore sediment was resuspended in 150 ml extracted xylem sap of *B. napus*; SXM, the minimal medium Czapek-Dox medium (CDM, modified from [58] and [59]) supplemented with 7% extracted xylem sap or plant proteins; H_2O and H_2O supplemented with 0.1% glucose; YNB (yeast nitrogen base: 1.5 g/l YNB, 5 g/l $(NH_4)_2SO_4$, 20 g/l glucose, ad 1 l H_2O) and vegetable juice (V8, Campbell Soup Company). After an additional incubation period of four days, proteins of the supernatant were precipitated with TCA/acetone.

Xylem sap extraction

Xylem sap was extracted from *B. napus* (Falcon, Norddeutsche Pflanzensucht). Seeds were surface sterilized with 70% ethanol and sown on sand. Plants were grown at long-day condition (16h light: 8h dark) and 22°C. Seven-day-old seedlings were transferred into a soil/sand (1: 1) mixture and grown for 42 days. To extract the xylem sap, plants were cut at the height of the first internode and the xylem sap was collected. The xylem sap was filtered through Vivaspin 15R centrifugal concentrators (Sartorius) and directly used as medium for inoculation.

626 **Genomic DNA Extraction**

627 For isolation of genomic DNA (gDNA) from fungal powder, the method modified from
628 [60] was used. The fine powder was mixed with 800 µl of lysis buffer (50 mM Tris
629 (pH 7.5), 50 mM EDTA (pH 8), 3% (w/v) SDS and 1% (v/v) ß-mercaptoethanol) and
630 incubated at 65°C for one hour. Before the mixture was centrifuged for 20 min at
631 13000 rpm, 800 µl phenol were added. The upper aqueous phase was transferred to
632 a new tube. To denature the proteins, 500 µl chloroform were added, mixed and
633 centrifuged for 10 min at 13000 rpm. The upper phase was mixed with 400 µl of
634 isopropanol for precipitation of gDNA and centrifuged for 2 min at 13000 rpm. The
635 sedimented gDNA was washed with 70% (v/v) ethanol. The gDNA was dried at 65°C
636 for approximately 25 min before it was dissolved in up to 100 µl deionized H_2O
637 containing 2 µl RNase A (10 mg/ml) and treated at 65°C for 30 min to remove RNA.
638
639 **Plasmid and strain construction**
640 The desired genes and flanking regions for plasmid construction were amplified of
641 *V. dahliae* JR2 WT gDNA with the Phusion High Fidelity Polymerase, *Taq* DNA
642 Polymerase (both Thermo Fisher Scientific) or Q5 High Fidelity Polymerase (New
643 England Biolabs). Primers are listed in S6 Table.
644 GeneArt Seamless Cloning and Assembly Kit (Thermo Fisher Scientific) was used for
645 the cloning strategy. Plasmids are listed in S7 Table. *E. coli* strain DH5α was utilized
646 for cloning reactions and propagation of plasmids. Transformation of *E. coli* was
647 performed based on a heat shock method [61]. *A. tumefaciens* AGL-1 cells were
648 transformed with the desired plasmids via a freeze-thaw method [62] and was then
649 utilized for an *A. tumefaciens* mediated transformation of *V. dahliae* spores, which was
650 performed based on the method described by [63]. Details on specific mutant strains
651 in haploid *V. dahliae* are given in S1 Text.

652

653 **Southern hybridization analysis**

654 For verification of *V. dahliae* deletion strains, the corresponding flanking region of the
655 gene was amplified and labeled as probe. Genomic DNAs were restricted with
656 indicated enzymes overnight. The mixture was separated on a 1% agarose gel, and
657 DNA was transferred to a Hybond-N membrane (GE Healthcare) by blotting. DNA on
658 the membrane was hybridized overnight to the probe. CDP-Star Detection reagent (GE
659 Healthcare) was used to detect chemiluminescence signals according to the
660 manufacturer's instructions.

661

662 **Protein assays and western hybridization analysis**

663 Extracellular proteins from the supernatant of SXM cultures were precipitated with
664 10% TCA (w/v) in acetone at 4°C overnight. This mixture was centrifuged at 4 000 rpm
665 for 60 min at 4°C. The protein sediment was washed three times with 80% (v/v)
666 acetone, once with 100% (v/v) acetone and then dissolved in 8 M urea/ 2 M thiourea.
667 Intracellular proteins were extracted from ground mycelium with extraction buffer
668 (300 mM NaCl, 100 mM Tris-HCl pH 7.5, 10% glycerol, 1 mM EDTA, 0.02% NP-40,
669 2 mM DTT and complete EDTA-free protease inhibitor cocktail (Roche)). Samples
670 were centrifuged for 20 min at 13 000 rpm at 4°C and the supernatants were
671 transferred into fresh test tubes. Protein concentrations were determined using a
672 Bradford-based Roti-Quant assay (Carl Roth). Protein samples were separated in 12%
673 SDS-PAGE gels, followed by protein transfer onto an Amersham Protran 0.45 µm
674 nitrocellulose membrane (GE Healthcare). The membrane was blocked in 5% (w/v)
675 skim milk powder in TBS-T (10 mM Tris-HCl (pH 8), 150 mM NaCl, 0.05% (w/v) Tween
676 20) and probed with α-GFP antibody (Santa Cruz Biotechnology). As secondary
677 antibody the horseradish peroxidase-coupled α-mouse antibody (115-035-003,

678 Jackson ImmunoResearch) was applied. Detection of chemiluminescent signals was
679 conducted with horseradish peroxidase substrate luminol based chemiluminescence.
680
681 **Tryptic digestion, mass spectrometry analysis and protein identification**
682 For one-dimensional gel analysis 30 µg of the extracellular protein extract was
683 separated by 12% SDS-PAGE gels. The polyacrylamide gels were incubated 1h in
684 fixing solution (40% (v/v) ethanol, 10% (v/v) acetic acid) and washed twice for 20 min
685 with H_2O. Gels were colloidal Coomassie stained (0.12% (w/v) CBB G-250, 5% (w/v)
686 aluminum sulphate-(14-18)-hydrate, 10% (v/v) methanol, 2% (v/v) orthophosphoric
687 acid (85%)) and two lanes for each growth condition were cut into ten pieces of equal
688 size. The excised polyacrylamide gels were in-gel digested with trypsin [64]. Resulting
689 tryptic peptide mixtures were separated by a reversed-phase liquid chromatographic
690 column (Acclaim PepMap RSLC column, 75 µm x 15 cm, C18, 3 µm, 100 Å,
691 P/N164534, Thermo Fisher Scientific) to further reduce sample complexity prior to
692 mass analyses with an LTQ Velos Pro mass spectrometer (Thermo Fisher Scientific).
693 To identify matches of the detected peptides an in-house genome-wide protein
694 sequence database of *Verticillium longisporum* was used of which the protein
695 sequences are given in S1 Table. Analysis was performed by a Thermo Proteome
696 Discoverer (version 1.3) workflow that integrates Sequest and Mascot search engines.
697 For the search an initial precursor mass tolerance of 10 ppm and fragment mass
698 tolerance of 0.8 Da Carbamidomethylcysteine was used as fixed modification.
699 Oxidized methionine was included as variable modification and two miscleavages were
700 allowed for each peptide. For peptide and protein validation, a 0.5% false discovery
701 rate was set and determined by using peptide validator with a reverse decoy database.
702 Resulting lists of identified proteins were semi-quantitatively processed using the
703 Marvis Suite software [34]. Only proteins with a WoLF PSORT extracellular localization

prediction of above 12 were considered for further characterization [65]. A group of 445 identified proteins fulfilled the criteria of a threshold of 1 peptide and a high intensity ratio of 0.83 in one condition. The protein sequences of the 445 proteins, and details on their abundance as measured by identified peptides, are given in S1 Table. The signal-to-level (s/l) ratio (see MarVis-Suite handbook on http://marvis.gobics.de) was calculated using as signal the difference between SXM and xylem sap condition averages (or vice versa) and as level the corresponding maximum. Polypeptides with an s/l ratio above 0.3 were considered as candidates with higher intensities in the specific medium and therefore belong to the specifically enriched proteins. Xylem sap-specific proteins are depicted in green and SXM-specific proteins in red. Whereas an s/l ratio below 0.3 was considered not to be specifically enriched and formed the shared core proteome.

The list of proteins was further analyzed and compared to the Ensembl Fungi annotations which are more robust. Candidates with no proper predictions in our preliminary genome-wide protein sequence database of *V. longisporum* (e.g. stop codons in protein sequences, two genes annotated as one) were revealed by comparison with corresponding *V. dahliae* JR2 and *V. alfalfae* VaMs.102 sequences and eliminated from the list. Further analyses are based on the *V. dahliae* JR2 or the *V. alfalfae* VaMs.102 protein sequences [35]. Domain predictions and associated families were obtained with InterProScan [36] and classification of carbohydrate-active enzyme (CAZys) families according to the CAZy database (http://www.cazy.org) was specified with dbCAN2 [37] to address putative functions of the proteins. Proteins were considered as putatively secreted with at least one predicted signal peptide by InterProScan [36] or SignalP-5.0 [66] or as long as it passed the threshold of 12 as determined by WoLF PSORT [65] for the *V. longisporum* 43, *V. dahliae* JR2 or *V. alfalfae* VaMs.102 protein sequence. All details are given in S2 Table.

730

731 **_A. thaliana_ root infection assay**

732 *A. thaliana* (Col-0, N1902; Nottingham Arabidopsis Stock Centre) seedlings were
733 inoculated by root-dipping with a conidia suspension of *V. dahliae* JR2 and *NLP3*
734 deletion strain overexpressing *GFP* (1×10^7 spores/ml) based on the method described
735 by colleagues [53]. Three-week-old seedlings were used for infection. The roots were
736 incubated in spore solutions with 100 000 spores/ml for 35 minutes. The plates were
737 further incubated in the plant chamber at long day conditions (22-25°C) and
738 colonization on the roots was monitored at indicated time points. The root was
739 incubated in a staining solution (0.0025% (v/v) propidium iodide, 0.005% (v/v) silwet)
740 for five minutes in the dark. Images of infected roots were taken with a Zeiss Observer
741 Z1 microscope equipped with CSU-X1 A1 confocal scanner unit (Yokogawa),
742 QuandtEM:512SC (Photometrics) digital camera and Slidebook 5.0 software package
743 (Intelligent Imaging Innovations).

744

745 **Tomato infection assay**

746 *Solanum lycopersicum* (Moneymaker, Bruno Nebelung Kiepenkerl-
747 Pflanzenzüchtung) seeds were surface sterilized with 70% (v/v) EtOH, 0.05%
748 Tween 20, sown on sand/soil (1:1) mixture (Dorsilit, Archut). Plants were grown under
749 a photoperiod of 16 h light and 8 h of darkness at 25 and 22°C, respectively. The
750 tomato pathogenicity assays were performed on ten-day-old *S. lycopersicum*
751 seedlings. The plants were root-inoculated by incubating the roots in 50 ml of 10^7
752 spores/ml for 40 min under constant agitation at ~35 rpm. Mock control plants were
753 treated similarly with dH_2O.

754 The seedlings were transferred to pots containing a sand/soil (1:1) mixture and
755 3 000 000 spores or 3 ml dH_2O for mock plants were added to the soil. For each strain

or control 15 plants were infected. Plants were incubated in the climate chamber at long day conditions for another 21 days before disease symptoms were scored. The fresh weight of the aerial parts, the length of the longest leaf and the height of the vegetation point were measured. These parameters were calculated into a disease score ranking relative to uninfected mock plants. The mean values of mock plants of each parameter were set to 100%. All values above 80% were assigned as 'healthy', 60-80% as 'mild symptoms', 40-80% as 'strong symptoms', lower than 40% as 'very strong symptoms' and dead plants as 'dead'. The scores for each strain were visualized in a stack diagram displaying the number of plants per disease score relative to the total amount of tested plants from all experiments. As another measure the discoloration of the tomato hypocotyl was observed with a binocular microscope SZX12-ILLB2-200 from Olympus. All treated plants were tested for fungal outgrowth 21 days after infection. The tomato stems were surface sterilized in 70% ethanol, followed by 6% hypochlorite solution each for 8 min before two washing steps with dH_2O. Stem ends were removed and slices were placed on PDM plates containing 100 µg/ml chloramphenicol. After incubation of seven days at 25°C the fungal outgrowth was observed. The pathogenicity assay was performed once with the metalloprotease constructs and once with Δ*GLA1*, Δ*CBD1* and Δ*AMY1* strains. Pathogenicity assays with the *CP* and *NLP* constructs were repeated twice. For each assay 15 plants were infected with WT and 15 plants were used as mock control. Per transformant 15 plants were infected and scores of identical strains were taken together of two individual transformants.

Accession numbers

Sequence data for *V. dahliae* were retrieved from Ensembl Fungi with the following accession numbers: *NLP2* (*VDAG_JR2_Chr2g05460a*), *NLP3*

(*VDAG_JR2_Chr4g05950a*), *CP1* (*VDAG_JR2_Chr7g00860a*), *CP2* (*VDAG_JR2_Chr2g07000a*), *MEP1* (VDAG_JR2_Chr8g09760a), *MEP2* (VDAG_JR2_Chr1g21900a), *GLA1* (*VDAG_JR2_Chr8g11020a*), *CBD1* (*VDAG_JR2_Chr4g04440a*), *AMY1* (*VDAG_JR2_Chr7g03330a*). Protein sequences for *V. longisporum* are given in S1 Table as retrieved from an in-house database or taken from Ensembl Fungi.

Acknowledgments

The authors thank N. Scheiter for technical assistance and A. Keyl and A. Pelizaeus for help with the experimental work during lab rotations. This research has been funded by the German Research Foundation (DFG, IRTG 2172 “PRoTECT” program of the Göttingen Graduate Center of Neurosciences, Biophysics, and Molecular Biosciences) to ML, JS, IM, AN, GHB, and IF, the Federal Ministry of Education and Research (BMBF “BioFung”, FKZ 0315595) to AK, ML, SB-S, GHB, BM and IF and an NSERC CREATE award to JWK.

References

1. Klosterman SJ, Atallah ZK, Vallad GE, Subbarao KV. Diversity, pathogenicity, and management of *Verticillium* species. Annu Rev Phytopathol. 2009. 47: 39–62.
2. Inderbitzin P, Subbarao KV. *Verticillium* systematics and evolution: how confusion impedes Verticillium wilt management and how to resolve it. Phytopathology. 2014. 104: 564–574.
3. Dunker S, Keunecke H, Steinbach P, von Tiedemann A. Impact of *Verticillium longisporum* on yield and morphology of winter oilseed rape (*Brassica napus*) in relation to systemic spread in the plant. J Phytopathol. 2008. 156: 698–707.
4. Eynck C, Koopmann B, Grunewaldt-Stoecker G, Karlovsky P, von Tiedemann A. Differential interactions of *Verticillium longisporum* and *V. dahliae* with *Brassica napus* detected with molecular and histological techniques. Eur J Plant Pathol. 2007. 118: 259–274.
5. Fradin EF, Thomma BPHJ. Physiology and molecular aspects of Verticillium wilt diseases caused by *V. dahliae* and *V. albo-atrum*. Mol Plant Pathol. 2006. 7: 71–86.
6. de Boer AH, Volkov V. Logistics of water and salt transport through the plant: structure and functioning of the xylem. Plant, Cell Environ. 2003. 26: 87–101.
7. Singh S, Braus-Stromeyer SA, Timpner C, Tran VT, Lohaus G, Reusche M, et al. Silencing of *Vlaro2* for chorismate synthase revealed that the phytopathogen *Verticillium longisporum* induces the cross-pathway control in the xylem. Appl Microbiol Biotechnol. 2010. 85: 1961–1976.
8. Carella P, Wilson DC, Kempthorne CJ, Cameron RK. Vascular sap proteomics: Providing insight into long-distance signaling during stress. Front Plant Sci. 2016. 7: 651.

9. Floerl S, Druebert C, Majcherczyk A, Karlovsky P, Kües U, Polle A. Defence reactions in the apoplastic proteome of oilseed rape (*Brassica napus* var. *napus*) attenuate *Verticillium longisporum* growth but not disease symptoms. BMC Plant Biol. 2008. 8: 129.

10. Timpner C, Braus-Stromeyer SA, Tran VT, Braus GH. The Cpc1 regulator of the cross-pathway control of amino acid biosynthesis Is required for pathogenicity of the vascular pathogen *Verticillium longisporum*. Mol Plant-Microbe Interact. 2013. 26: 1312–1324.

11. Isshiki A, Akimitsu K, Yamamoto M, Yamamoto H. Endopolygalacturonase is essential for citrus black rot caused by *Alternaria citri* but not brown spot caused by *Alternaria alternata*. Mol Plant-Microbe Interact. 2001. 14: 749–757.

12. Yakoby N, Beno-Moualem D, Keen NT, Dinoor A, Pines O, Prusky D. *Colletotrichum gloeosporioides pel*B is an important virulence factor in avocado fruit-fungus interaction. Mol Plant-Microbe Interact. 2001. 14: 988–995.

13. Oeser B, Heidrich PM, Müller U, Tudzynski P, Tenberge KB. Polygalacturonase is a pathogenicity factor in the *Claviceps purpurea*/rye interaction. Fungal Genet Biol. 2002. 36: 176–186.

14. Voigt CA, Schäfer W, Salomon S. A secreted lipase of *Fusarium graminearum* is a virulence factor required for infection of cereals. Plant J. 2005. 42: 364–375.

15. Brito N, Espino JJ, González C. The endo-beta-1,4-xylanase xyn11A is required for virulence in *Botrytis cinerea*. Mol Plant-Microbe Interact. 2006. 19: 25–32.

16. Sorrell TC, Chen SCA. Fungal-derived immune modulating molecules. In: Fallon PG (ed) Pathogen-derived immunomodulatory molecules. Advances in Experimental Medicine and Biology. New York, NY: Springer, 2009, pp. 108–120.

17. Dodds PN, Rathjen JP. Plant immunity: towards an integrated view of plant–

849 pathogen interactions. Nat Rev Genet. 2010. 11: 539–548.
850 18. Lo Presti L, Lanver D, Schweizer G, Tanaka S, Liang L, Tollot M, et al. Fungal
851 effectors and plant susceptibility. Annu Rev Plant Biol. 2015. 66: 513–545.
852 19. van Esse HP, Bolton MD, Stergiopoulos I, de Wit PJGM, Thomma BPHJ. The
853 chitin-binding *Cladosporium fulvum* effector protein Avr4 is a virulence factor.
854 Mol Plant-Microbe Interact. 2007. 20: 1092–1101.
855 20. de Jonge R, van Esse HP, Kombrink A, Shinya T, Desaki Y, Bours R, et al.
856 Conserved fungal LysM effector Ecp6 prevents chitin-triggered immunity in
857 plants. Science. 2010. 329: 953–955.
858 21. Volk H, Marton K, Flajšman M, Radišek S, Tian H, Hein I, et al. Chitin-binding
859 protein of *Verticillium nonalfalfae* disguises fungus from plant chitinases and
860 suppresses chitin-triggered host immunity. Mol Plant-Microbe Interact. 2019. 32:
861 1378–1390.
862 22. Zhang Y, Gao Y, Liang Y, Dong Y, Yang X, Yuan J, et al. The *Verticillium dahliae*
863 SnodProt1-like protein VdCP1 contributes to virulence and triggers the plant
864 immune system. Front Plant Sci. 2017. 8: 1880.
865 23. Naumann TA, Wicklow DT, Price NPJ. Identification of a chitinase-modifying
866 protein from *Fusarium verticillioides*: truncation of a host resistance protein by a
867 fungalysin metalloprotease. J Biol Chem. 2011. 286: 35358–66.
868 24. Han LB, Li YB, Wang FX, Wang WY, Liu J, Wu JH, et al. The cotton apoplastic
869 protein CRR1 stabilizes chitinase 28 to facilitate defense against the fungal
870 pathogen *Verticillium dahliae*. Plant Cell. 2019. 31: 520–536.
871 25. Gijzen M, Nürnberger T. Nep1-like proteins from plant pathogens: Recruitment
872 and diversification of the NPP1 domain across taxa. Phytochemistry. 2006. 67:
873 1800–1807.
874 26. Santhanam P, van Esse HP, Albert I, Faino L, Nürnberger T, Thomma BPHJ.

875 Evidence for functional diversification within a fungal NEP1-like protein family.
876 Mol Plant-Microbe Interact. 2013. 26: 278–286.
877 27. Zhou BJ, Jia PS, Gao F, Guo HS. Molecular characterization and functional
878 analysis of a necrosis-and ethylene-inducing, protein-encoding gene family from
879 *Verticillium dahliae*. Mol Plant-Microbe Interact. 2012. 25: 964–975.
880 28. Marton K, Flajsman M, Radisek S, Kosmelj K, Jakse J, Javornik B, et al.
881 Comprehensive analysis of *Verticillium nonalfalfae in silico* secretome uncovers
882 putative effector proteins expressed during hop invasion. PLoS One. 2018. 13:
883 e0198971.
884 29. Klosterman SJ, Subbarao KV., Kang S, Veronese P, Gold SE, Thomma BPHJ,
885 et al. Comparative genomics yields insights into niche adaptation of plant
886 vascular wilt pathogens. PLoS Pathog. 2011. 7: e1002137.
887 30. Yellareddygari SKR, Gudmestad NC. Effect of soil temperature, injection depth,
888 and rate of metam sodium efficacy in fine-textured soils with high organic matter
889 on the management of Verticillium wilt of potato. Am J Potato Res. 2018. 95:
890 413–422.
891 31. Singh S, Braus-Stromeyer SA, Timpner C, Valerius O, von Tiedemann A,
892 Karlovsky P, et al. The plant host *Brassica napus* induces in the pathogen
893 *Verticillium longisporum* the expression of functional catalase peroxidase which
894 is required for the late phase of disease. Mol Plant-Microbe Interact. 2012. 25:
895 569–581.
896 32. Neumann MJ, Dobinson KF. Sequence tag analysis of gene expression during
897 pathogenic growth and microsclerotia development in the vascular wilt pathogen
898 *Verticillium dahliae*. Fungal Genet Biol. 2003. 38: 54–62.
899 33. Mandelc S, Javornik B. The secretome of vascular wilt pathogen *Verticillium*
900 *albo-atrum* in simulated xylem fluid. Proteomics. 2015. 15: 787–797.

34. Kaever A, Landesfeind M, Possienke M, Feussner K, Feussner I, Meinicke P. MarVis-filter: Ranking, filtering, adduct and isotope correction of mass spectrometry data. J Biomed Biotechnol. 2012. 2012: 263910.

35. Kersey PJ, Allen JE, Allot A, Barba M, Boddu S, Bolt BJ, et al. Ensembl Genomes 2018: An integrated omics infrastructure for non-vertebrate species. Nucleic Acids Res. 2018. 46: D802–D808.

36. Jones P, Binns D, Chang HY, Fraser M, Li W, McAnulla C, et al. InterProScan 5: Genome-scale protein function classification. Bioinformatics. 2014. 30: 1236–1240.

37. Zhang H, Yohe T, Huang L, Entwistle S, Wu P, Yang Z, et al. dbCAN2: A meta server for automated carbohydrate-active enzyme annotation. Nucleic Acids Res. 2018. 46: W95–W101.

38. Lombard V, Golaconda Ramulu H, Drula E, Coutinho PM, Henrissat B. The carbohydrate-active enzymes database (CAZy) in 2013. Nucleic Acids Res. 2014. 42: D490-495.

39. Yang Y, Zhang Y, Li B, Yang X, Dong Y, Qiu D. A *Verticillium dahliae* pectate lyase induces plant immune responses and contributes to virulence. Front Plant Sci. 2018. 9: 1271.

40. Gui YJ, Chen JY, Zhang DD, Li NY, Li TG, Zhang WQ, et al. *Verticillium dahliae* manipulates plant immunity by glycoside hydrolase 12 proteins in conjunction with carbohydrate-binding module 1. Environ Microbiol. 2017. 19: 1914–1932.

41. Wang JY, Cai Y, Gou JY, Mao YB, Xu YH, Jiang WH, et al. VdNEP, an elicitor from *Verticillium dahliae*, induces cotton plant wilting. Appl Environ Microbiol. 2004. 70: 4989–4995.

42. McCotter SW, Horianopoulos LC, Kronstad JW. Regulation of the fungal secretome. Curr Genet. 2016. 62: 533–545.

927 43. Yadeta KA, J. Thomma BPH. The xylem as battleground for plant hosts and
928 vascular wilt pathogens. Front Plant Sci. 2013. 4: 97.
929 44. Scholz SS, Schmidt-Heck W, Guthke R, Furch ACU, Reichelt M, Gershenzon J,
930 et al. *Verticillium dahliae-Arabidopsis* interaction causes changes in gene
931 expression profiles and jasmonate levels on different time scales. Front
932 Microbiol. 2018. 9: 217.
933 45. Mösch HU, Scheier B, Lahti R, Mäntsälä P, Braus GH. Transcriptional activation
934 of yeast nucleotide biosynthetic gene *ADE4* by GCN4. J Biol Chem. 1991. 266:
935 20453–20456.
936 46. Hoffmann B, Valerius O, Andermann M, Braus GH. Transcriptional
937 autoregulation and inhibition of mRNA translation of amino acid regulator gene
938 *cpcA* of filamentous fungus *Aspergillus nidulans*. Mol Biol Cell. 2001. 12: 2846–
939 2857.
940 47. Jiménez-Ruiz J, Leyva-Pérez M de la O, Cabanás CGL, Barroso JB, Luque F,
941 Mercado-Blanco J. The transcriptome of *Verticillium dahliae* responds
942 differentially depending on the disease susceptibility level of the olive (*Olea*
943 *europaea* L.) cultivar. Genes (Basel). 2019. 10: 251.
944 48. Jin L, Chen D, Liao S, Zhang Y, Yu F, Wan P, et al. Transcriptome analysis
945 reveals downregulation of virulence-associated genes expression in a low
946 virulence *Verticillium dahliae* strain. Arch Microbiol. 2019. 201: 927–941.
947 49. Seidl MF, Cook DE, Thomma BPHJ. Chromatin biology impacts adaptive
948 evolution of filamentous plant pathogens. PLoS Pathog. 2016. 12: e1005920.
949 50. Tan KC, Oliver RP. Regulation of proteinaceous effector expression in
950 phytopathogenic fungi. PLoS Pathog. 2017. 13: e1006241.
951 51. Soyer JL, El Ghalid M, Glaser N, Ollivier B, Linglin J, Grandaubert J, et al.
952 Epigenetic control of effector gene expression in the plant pathogenic fungus

Leptosphaeria maculans. PLoS Genet. 2014. 10: e1004227.

52. Tran VT, Braus-Stromeyer SA, Kusch H, Reusche M, Kaever A, Kühn A, et al. *Verticillium* transcription activator of adhesion Vta2 suppresses microsclerotia formation and is required for systemic infection of plant roots. New Phytol. 2014. 202: 565–581.

53. Bui T, Harting R, Braus-Stromeyer SA, Tran V, Leonard M, Höfer A, et al. *Verticillium dahliae* transcription factors Som1 and Vta3 control microsclerotia formation and sequential steps of plant root penetration and colonisation to induce disease. New Phytol. 2019. 221: 2138–2159.

54. Jashni MK, Dols IHM, Iida Y, Boeren S, Beenen HG, Mehrabi R, et al. Synergistic action of a metalloprotease and a serine protease from *Fusarium oxysporum* f. sp. *lycopersici* cleaves chitin-binding tomato chitinases, reduces their antifungal activity, and enhances fungal virulence. Mol Plant-Microbe Interact. 2015. 28: 996–1008.

55. Brouta F, Descamps F, Monod M, Vermout S, Losson B, Mignon B. Secreted metalloprotease gene family of *Microsporum canis*. Infect Immun. 2002. 70: 5676–5683.

56. Naumann TA, Price NPJ. Truncation of class IV chitinases from *Arabidopsis* by secreted fungal proteases. Mol Plant Pathol. 2012. 13: 1135–1139.

57. Hollensteiner J, Wemheuer F, Harting R, Kolarzyk AM, Diaz Valerio SM, Poehlein A, et al. *Bacillus thuringiensis* and *Bacillus weihenstephanensis* inhibit the growth of phytopathogenic *Verticillium* species. Front Microbiol. 2017. 7: 2171.

58. Czapek F. Untersuchungen über die Stickstoffgewinnung und Eiweißbildung der Pflanzen. Beiträge zur Chem Physiol und Pathol 1. 1902. 1: 538–560.

59. Dox AW. The intracellular enzyms of *Penicillium* and *Aspergillus*, with special

979 references to those of *Penicillium camemberti*. Washington, D.C.: U.S. Dept. of
980 Agriculture, Bureau of Animal Industry, 1910.
981 60. Kolar M, Punt PJ, van den Hondel CAMJJ, Schwab H. Transformation of
982 *Penicillium chrysogenum* using dominant selection markers and expression of
983 an *Escherichia coli lacZ* fusion gene. Gene. 1988. 62: 127–134.
984 61. Inoue H, Nojima H, Okayama H. High efficiency transformation of *Escherichia*
985 *coli* with plasmids. Gene. 1990. 96: 23–28.
986 62. Jyothishwaran G, Kotresha D, Selvaraj T, Srideshikan SH, Rajvanshi PK,
987 Jayabaskaran C. A modified freeze–thaw method for efficient transformation of
988 *Agrobacterium tumefaciens*. Curr Sci. 2007. 93: 770–772.
989 63. Mullins ED, Chen X, Romaine P, Raina R, Geiser DM, Kang S. *Agrobacterium*-
990 mediated transformation of *Fusarium oxysporum*: An efficient tool for insertional
991 mutagenesis and gene transfer. Phytopathology. 2001. 91: 173–180.
992 64. Shevchenko A, Wilm M, Vorm O, Mann M. Mass spectrometric sequencing of
993 proteins from silver-stained polyacrylamide gels. Anal Chem. 1996. 68: 850–
994 858.
995 65. Horton P, Park KJ, Obayashi T, Fujita N, Harada H, Adams-Collier CJ, et al.
996 WoLF PSORT: Protein localization predictor. Nucleic Acids Res. 2007. 35:
997 W585–W587.
998 66. Almagro Armenteros JJ, Tsirigos KD, Sønderby CK, Petersen TN, Winther O,
999 Brunak S, et al. SignalP 5.0 improves signal peptide predictions using deep
1000 neural networks. Nat Biotechnol. 2019. 37: 420–423.
1001 67. Meinicke P, Lingner T, Kaever A, Feussner K, Göbel C, Feussner I, et al.
1002 Metabolite-based clustering and visualization of mass spectrometry data using
1003 one-dimensional self-organizing maps. Algorithms Mol Biol. 2008. 3: 9.
1004

Figures

Fig 1. Exoproteome signatures of *V. longisporum* in different growth media.

V. longisporum 43 was cultivated in complete medium (PDM) for four days before the sedimented mycelia and spores were dissolved in different media (dH_2O, dH_2O + 0.1% glucose, yeast nitrogen base (YNB), vegetable juice (V8), minimal medium (CDM) supplemented with 7% xylem sap or plant proteins, simulated xylem medium (SXM) and extracted xylem sap from *B. napus*) and cultivated for four more days. **(A)** Precipitated proteins from the supernatants were separated by one-dimensional SDS-PAGE. The colloidal Coomassie stained exoproteome samples on gel displayed a strong variation between the protein band distributions of all different culture conditions. Lanes M represent the molecular weight marker. Complete lanes of the *V. longisporum* exoproteomes were subjected to tryptical protein digestion and the resulting peptides were analyzed by LC MS/MS. **(B)** Clustering analysis of protein abundances (spectral counts) was facilitated by the software MarVis and is visualized as one-dimensional self-organizing maps. Rows represent the compared growth conditions. The spectral counts were normalized and color-coded according to the indicated scale. Red indicates increased, dark blue no spectral counts. **(C)** The principle component analysis plot of the exoproteomes based on the spectral counts was performed with MarVis-software [67]. Each dot represents one biological replicate (one independent culture). The compared exoproteome signatures cluster in three groups: a first cluster is formed by all xylem sap culture samples (blue circle); the second cluster contains all SXM culture samples (red circle) and the third cluster consists of all other samples (black circle).

Fig 2. Comparison of exoproteome signatures for *V. longisporum* growth in xylem sap and pectin-rich simulated xylem medium.

Complete lanes of the SDS-gel with samples of *V. longisporum* simulated xylem medium (SXM) and xylem sap derived exoproteomes were subjected to tryptical protein digestion and the resulting peptides were analyzed by LC MS/MS. The obtained raw data were searched with Proteome Discoverer Software 1.3™ against a draft genome-wide protein sequence database of *V. longisporum*. Lists of identified proteins were semi-quantitatively processed using MarVis-Suite [34]. Single proteins with identifiers are found in S1 Table. **(A)** Clustering analysis of protein abundances (spectral counts) is visualized as one-dimensional self-organizing maps, which was facilitated by the software MarVis. Upper and lower rows represent the two compared growth conditions xylem sap and pectin-rich SXM, respectively. Each column corresponds to spectral counts of one identified protein. The spectral counts were normalized and color-coded according to the indicated scale. Red indicates increased, dark blue no spectral counts. **(B-E)** BLAST searches of identified *V. longisporum* proteins in **A** against the *V. dahliae* JR2 and the *V. alfalfae* VaMs.102 proteomes from Ensembl Fungi [35] were conducted and functional analysis is based on the *V. dahliae* JR2 or *V. alfalfae* VaMs.102 protein sequences. **(B)** The Venn diagram displays the number of proteins specifically enriched in xylem sap (blue) and proteins enriched in SXM (red). All proteins below the statistical threshold form the core exoproteome that is similarly enriched in both media (violet). **(C)** The cake diagram shows the functional classification of the 399 identified secreted proteins into main protein groups according to their predicted domains. **(D)** The functional groups are presented with the number of identified proteins in the different cultivation environments. **(E)** Classification by CAZy modules is shown for each cultivation type.

Fig 3. Exoproteins specifically secreted in xylem sap are dispensable for *V. dahliae ex planta* phenotype.

The same number of spores of *V. dahliae* JR2 wildtype (WT) and indicated deletion mutant (Δ*CP1*, ΔCP2, Δ*CP1/2*, Δ*NLP2*, Δ*NLP3*, Δ*NLP2/3*, Δ*MEP1*, Δ*MEP2*, Δ*MEP1/2*, Δ*GLA1*, Δ*CBD1*, Δ*AMY1*) and complementation (*CP1*-C, *CP2*-C) strains were point inoculated on simulated xylem medium (SXM) plates and incubated at 25°C for 10 days. For Δ*AMY1*, Δ*GLA1* and Δ*CBD1* mutants two transformants were spotted. Top-view scans of the colonies show a similar phenotype of all strains.

Fig 4. CAZys and metalloproteases specifically secreted in xylem sap are dispensable for *V. dahliae* pathogenicity on tomato.

Ten-day-old tomato seedlings were root-infected with spores of *V. dahliae* JR2 (WT) and the indicated single and double deletion strains (Δ*GLA1*, Δ*CBD1*, Δ*AMY1,* Δ*MEP1,* Δ*MEP2,* Δ*MEP1/2*). Uninfected plants (mock) served as control. The disease index was assessed after 21 days of growth in the climate chamber under 16h:8h light:dark at 22-25°C and includes the height of the plant, length of the 2nd true leaf and weight of the plant. Representative plants and discolorations of the hypocotyls are shown for each infection. The number (n) of plants is shown for each fungal strain or mock treatment. **(A)** Infections with *GLA1* (glycoamylase) deletion strains resulted in the same stunting phenotype as WT infections. **(B)** Strains with deletion of *CBD1* (carbohydrate-binding domain) or *AMY1* (amylase) resulted in a WT-like induction of disease symptoms. **(C)** Absence of metalloproteases Mep1 and Mep2 resulted in WT-like *V. dahliae* pathogenicity on tomato.

Fig 5. *V. dahliae* Cp1 and Cp2 are dispensable for virulence on tomato.

Ten-day-old tomato seedlings were infected by root-dipping in a spore suspension of *V. dahliae* JR2 (WT) and the indicated deletion (Δ*CP1*, ΔCP2, Δ*CP1/2*) and complementation strains (*CP1*-C, *CP2*-C). Plants were incubated in the climate

chamber under 16h:8h light:dark at 22-25°C. **(A)** The stack diagram shows the percentage of plants with the respective disease index. The disease index was assessed at 21 days post inoculation and includes the plant height, the longest leaf length and the fresh weight, which was compared to uninfected (mock) plants. The number (n) of treated plants is given for each fungal strain. **(B)** Representative plants, discolorations of the hypocotyls, and the fungal outgrowth of the stems are shown. The experiment was repeated twice. *CP1* and *CP2* deletion strains infect tomato plants to the same extent as WT and the complementation strains.

Fig 6. Nlp3-GFP is secreted into the extracellular space

V. dahliae JR2 (WT) ectopically overexpressing *GFP* (WT/OE-*GFP*) and WT and *NLP3* deletion strains ectopically overexpressing *NLP3-GFP* (WT/OE-*NLP3-GFP* and Δ*NLP3*/OE-*NLP3-GFP*, respectively) were tested for subcellular localization by fluorescence microscopy in **A** and localization and production of the intact full-length fusion protein intra- and extracellular by western hybridization in **B**. **(A)** Confocal microscopy of WT/OE-*NLP3-GFP* and Δ*NLP3*/OE-*NLP3-GFP* strains show the accumulation of the GFP signal inside the red-stained vacuoles whereas the strain WT/OE-*GFP* exhibits GFP signals in the cytoplasm. Spores of the indicated fungal strains were inoculated in 300 µl liquid PDM in µ-slide 8 well microcopy chambers (Ibidi) and incubated at 25°C overnight. Fungal hyphae were stained with the membrane-selective styryl dye *N*-(3-triethylammoniumpropyl)-4-(*p*-diethylaminophenyl-hexatrienyl) pyridinium dibromide (FM4-64). Scale bar = 10 µm. **(B)** Fungal strains grown in liquid simulated xylem medium (SXM) at 25°C for 24 hours. Western hybridization with α-GFP antibody was performed with 7 µg extracellular protein extracts from the culture supernatant and 50 µg intracellular protein extracts. Ponceau S staining served as loading control and WT was used as negative control.

Analysis of extracellular proteins in the supernatant of WT/OE-*NLP3-GFP* and Δ*NLP3*/OE-*NLP3-GFP* strains revealed strong signals for Nlp3-GFP with a size of 52 kDa whereas intracellular protein extracts result in faint bands at the size of the fusion protein as well as for free GFP (~27 kDa). In the control strain WT/OE-*GFP* a strong GFP signal was detected in intracellular extracts.

Fig 7. Necrosis and ethylene inducing-like effectors Nlp2 and Nlp3 contribute to *V. dahliae* virulence on tomato.

The *NLP3* deletion strain was tested for *A. thaliana* root colonization and single and double deletion strains of *NLP2* and *NLP3* were tested for pathogenicity on tomato. Infected plants were incubated in the climate chamber under 16h:8h light:dark at 22-25°C. **(A)** Three-week-old *A. thaliana* seedlings were root-infected with spores of *V. dahliae* JR2 and *NLP3* deletion strain overexpressing free GFP (WT/OE-*GFP* and Δ*NLP3*/OE-*GFP*, respectively). At three and five days post inoculation (dpi) the colonization of the fungal hyphae was monitored with root cells stained by 0.05% propidium iodide/0.01% silwet solution. The experiment was repeated twice with two individual transformants of Δ*NLP3*/OE-*GFP*. Fluorescence microscopy pictures show similar initial colonization of *V. dahliae* WT/OE-*GFP* and Δ*NLP3*/OE-*GFP* on the root surface at 3 dpi and whole root colonization at 5 dpi. 3D Surface views were generated by Slidebook 5.0 software from stacks of single pictures. Scale bar = 10 µm. **(B, C)** Ten-day-old tomato seedlings were root-infected with spores of *V. dahliae* JR2 and the indicated single *NLP2* (Δ*NLP2*) and *NLP3* (Δ*NLP3*) and *NLP2/3* double deletion strains (Δ*NLP2/3*). Uninfected plants (mock) served as control. Representative plants, discolorations of the hypocotyls, and the fungal outgrowth of the surface sterilized stems are shown. The disease index was assessed at 21 dpi, which shows that plants infected with *NLP2* and *NLP3* single and double deletion strains exhibit an intermediate

phenotype when compared with mock and WT-infected plants. The number of treated plants (n) is shown for each fungal strain. The experiment was repeated twice. For the deletion strains two individual transformants were tested.

Supporting information

S1 Fig. Verification of *V. dahliae NLP2* and *NLP3* deletion or overexpression constructs.

V. dahliae JR2 (WT) was transformed with the respective deletion cassettes to generate *NLP2* and *NLP3* deletion strains (Δ*NLP2* and Δ*NLP3*, respectively) via homologous recombination. The *NLP2/NLP3* double deletion strain (Δ*NLP2/3*) was obtained by transforming the Δ*NLP3* strain with the Δ*NLP2* construct. Strains overexpressing ectopically integrated *GFP* or *NLP3-GFP* were constructed by transforming WT or *NLP3* deletion strains with the displayed constructs (*GFP* and *NLP3-GFP* are driven by the *gpdA* promoter and followed by the *trpC* terminator). All constructs contain resistance cassettes (HYG^R: hygromycin resistance; NAT^R: nourseothricin resistance) with a *gpdA* promoter and a *trpC* terminator. Schemes with used restriction enzymes, corresponding cutting sites (arrows) and probes (red lines) used for Southern hybridization are presented in **A** and **B**. **(A)** *XhoI* and the 5' flanking region as probe were used for verification of the *NLP2* deletion strain. **(B)** Δ*NLP3* strain was confirmed using *Xho*I with 5' flanking region as probe. And ectopic integration of *GFP* into Δ*NLP3* strain and *NLP3-GFP* into WT or Δ*NLP3* strain was verified with restriction enzyme *Bgl*I with *GFP* as probe. **(C)** Confirmation of deletion strains by Southern hybridization is shown for Δ*NLP2* #4 = VGB390, #8 = VGB391; Δ*NLP3* #4 = VGB384, #5 = VGB385, Δ*NLP2/3* #6 = VGB400, #7 = VGB401; Δ*NLP3/*OE-*GFP* #8 = VGB431, #9 = VGB432, WT/OE-*NLP3-GFP* #2 = VGB407, #6 = VGB408, Δ*NLP3/*OE-*NLP3-GFP* #1 = VGB409, #7 = VGB410. Genomic WT DNA served as control. Restriction enzymes, probes and sizes of expected fragments are indicated.

S2 Fig. Verification of *V. dahliae CP1* and *CP2* deletion and complementation strains.

Deletion strains (Δ*CP1 and* Δ*CP2*) were obtained via homologous recombination between the deletion constructs and *V. dahliae* JR2 (WT). The *CP2* deletion strain was transformed with the *CP1* deletion construct to generate the double deletion strain Δ*CP1/2*. To generate ectopic complementation strains the constructs were integrated into the deletion strain as indicated by //. The constructs contain resistance cassettes (*HYG*^{R}: hygromycin resistance; *NAT*^{R}: nourseothricin resistance) controlled by the *gpdA* promoter and the *trpC* terminator. Schemes with used restriction enzymes, corresponding cutting sites (arrows) and probes (red lines) used for Southern hybridization are presented in **A** and **B**. **(A)** Confirmation of *CP1* deletion and complementation strain was achieved by enzyme restriction of gDNA with *Sal*I and 3' flanking region as probe or *Mfe*I and 5' flanking region as probe. **(B)** *Sma*I with 3' flanking region or *Hind*III with 5' flanking region as probe was used for *CP2* deletion and complementation strains. **(C)** Deletion and complementation strains were verified by Southern hybridization: Δ*CP1* #11 = VGB316, #13 = VGB317; *CP1*-C #6 = VGB489, #7 = VGB490; Δ*CP2* #4 = VGB406, #14 = VGB422; *CP2*-C #3 = VGB429, #7 = VGB430; Δ*CP1*Δ*CP2* #5 = VGB423, #10 = VGB424. Genomic WT DNA was used as control. Restriction enzymes, probes and sizes of expected fragments are depicted.

S3 Fig. Verification of *V. dahliae MEP1* and *MEP2* deletion strains.

MEP1 and *MEP2* deletion strains (Δ*MEP1* and Δ*MEP2*, respectively) were constructed via homologous recombination between the deletion construct and *V. dahliae* JR2 (WT) and confirmed by Southern hybridization. Restriction sites of used enzymes (arrows) and probes (red lines) used for Southern hybridization are depicted in **A** and **B**. **(A)** Deletion of *MEP1* was confirmed after enzyme restriction of gDNA with *Kpn*I or *Bgl*II and 3' flanking region as probe. *MEP1* deletion construct contains hygromycin resistance cassette (*HYG*^{R}) controlled by the *gpdA* promoter and the *trpC* terminator.

(B) Verification of *MEP2* deletion strain containing the nourseothricin resistance (*NAT*^{R}) cassette under control of the *gpdA* promoter and the *trpC* terminator was achieved with *Sac*I or *Nco*I restriction and 3' flanking region as probe. **(C)** Deletion strains were confirmed by Southern hybridization: Δ*MEP1* #7 = VGB226, #8 = VGB227; Δ*MEP2* #2 = VGB133, #8 = VGB126; Δ*MEP1/2* #2 = VGB204, #5 = VGB203. Genomic WT DNA served as control. Restriction enzymes, probes and sizes of expected fragments are indicated.

S4 Fig. Verification of *V. dahliae GLA1*, *CBD1* and *AMY1* deletion strains.

By homologous recombination between the deletion construct and *V. dahliae* JR2 (WT) the depicted deletion strains were obtained. The deletion constructs contain a nourseothricin resistance cassette (*NAT*^{R}) controlled by the *gpdA* promoter and the *trpC* terminator. The used probes (red lines) and restriction enzymes with their cutting sites (arrows) are illustrated in the schemes (left). The expected fragments were confirmed by Southern hybridization for each deletion strain with WT as control (right). **(A)** With *Xho*I and 5' flanking region as probe *GLA1* deletion strains (Δ*GLA1*) #4 = VGB129 and #10 = VGB131 were verified. **(B)** Verification of *CBD1* deletion strains (Δ*CBD1* #2 = VGB127, #5 = VGB132) was achieved with *Pvu*I enzyme restriction and 3' flanking region as probe and **(C)** *AMY1* deletion strains (Δ*AMY1* #2 = VGB130, #10 = VGB128) were verified with *Kpn*I and 3' flanking region as probe.

S5 Fig. Expression of *NLP3-GFP* under control of a constitutively active promoter allows *V. dahliae* wildtype-like growth on solid media.

50 000 spores of *V. dahliae* JR2 wildtype (WT) and *NLP3* deletion strains (Δ*NLP3*) and corresponding strains ectopically overexpressing *NLP3-GFP* (WT/*OE-NLP3-GFP* and Δ*NLP3*/*OE-NLP3-GFP*, respectively) were point inoculated on minimal medium (CDM)

plates. The growth phenotype was observed after 10 days of incubation at 25°C and revealed a similar phenotype for all tested strains.

S1 Table. List of identified proteins in SXM and xylem sap.

S2 Table. Annotation of identified proteins in SXM and xylem sap.

S3 Table. Functional groups of secreted proteins.

S4 Table. CAZy classification of secreted proteins.

S5 Table. *Verticillium* strains used in this study.

S6 Table. Primers used in this study.

S7 Table. Plasmids used in this study.

S1 Text. Additional Materials and Methods.

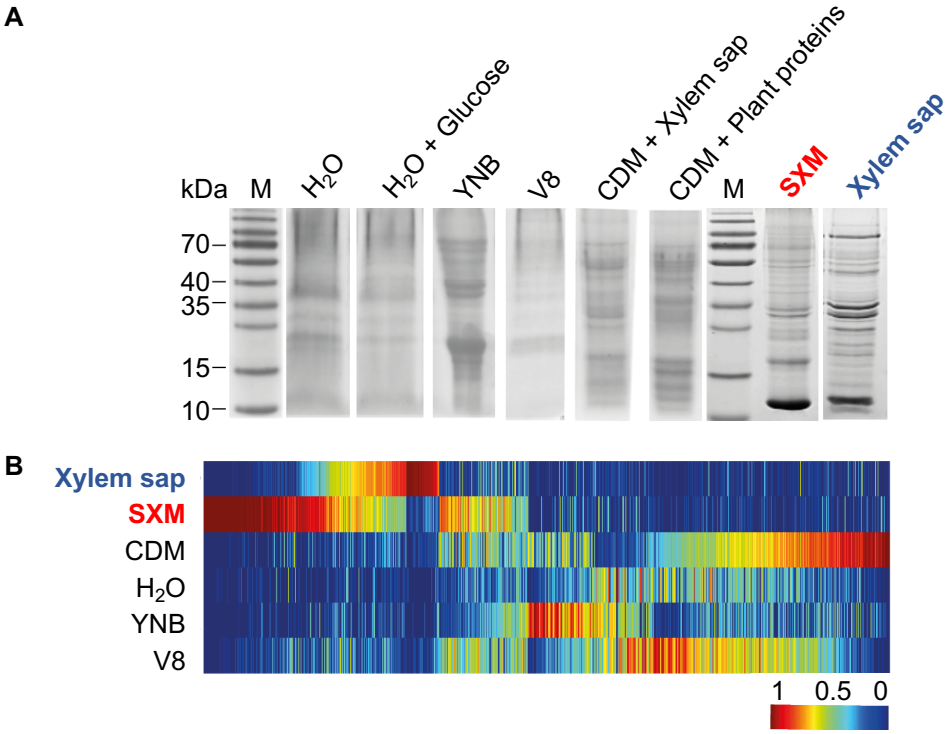
A
kDa
M
H2O
H2O + Glucose
YNB
V8
CDM + Xylem sap
CDM + Plant proteins
M
SXM
Xylem sap
70
40
35
15
10
B
Xylem sap
SXM
CDM
H2O
YNB
V8
1
0.5
0
C
SXM
H2O
CDM
YNB
V8
Xylem sap
PC2
PC1
15
10
5
0
-5
-10
-15
-15
-10
-5
0
5
10
15
20

Figure 1


A
SXM
Xylem sap
enriched in SXM
enriched in Xylem sap
1
0.5
0

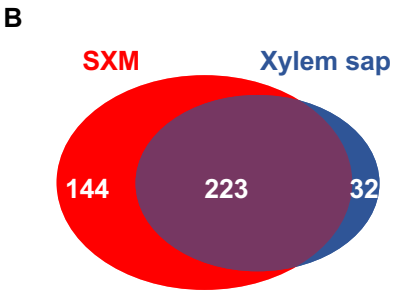
B
SXM
Xylem sap
144
223
32

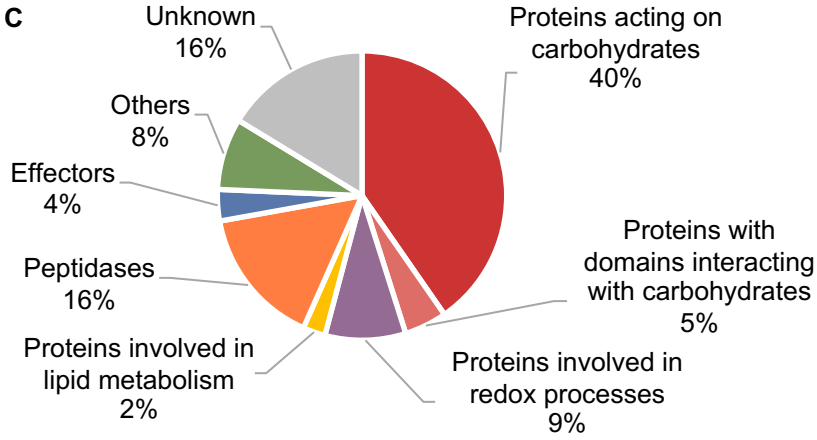
C
Unknown 16%
Proteins acting on carbohydrates 40%
Others 8%
Effectors 4%
Proteins with domains interacting with carbohydrates 5%
Peptidases 16%
Proteins involved in lipid metabolism 2%
Proteins involved in redox processes 9%

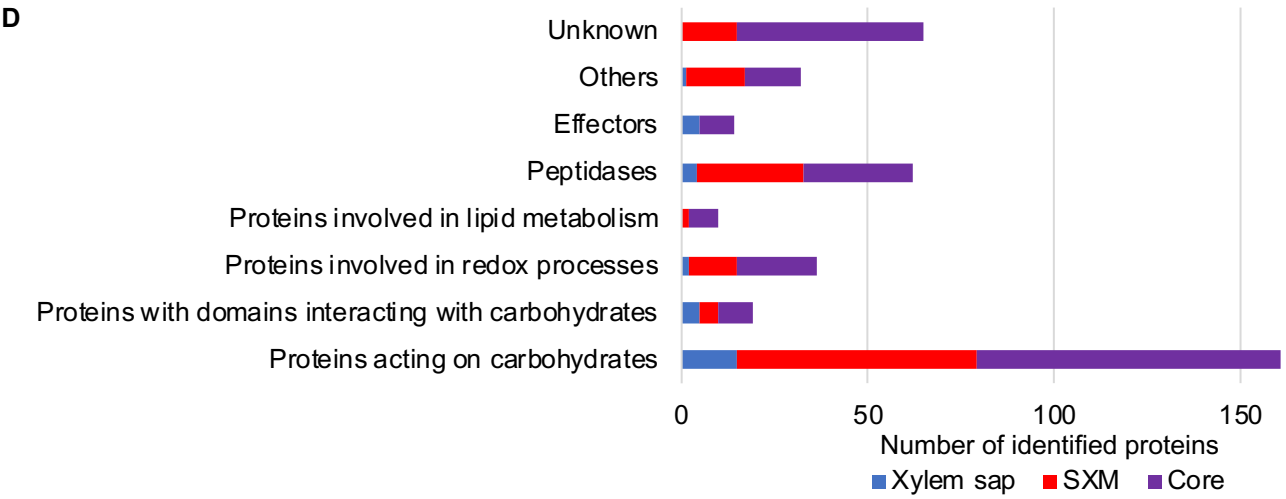
D
Unknown
Others
Effectors
Peptidases
Proteins involved in lipid metabolism
Proteins involved in redox processes
Proteins with domains interacting with carbohydrates
Proteins acting on carbohydrates
0
50
100
150
Number of identified proteins
Xylem sap
SXM
Core

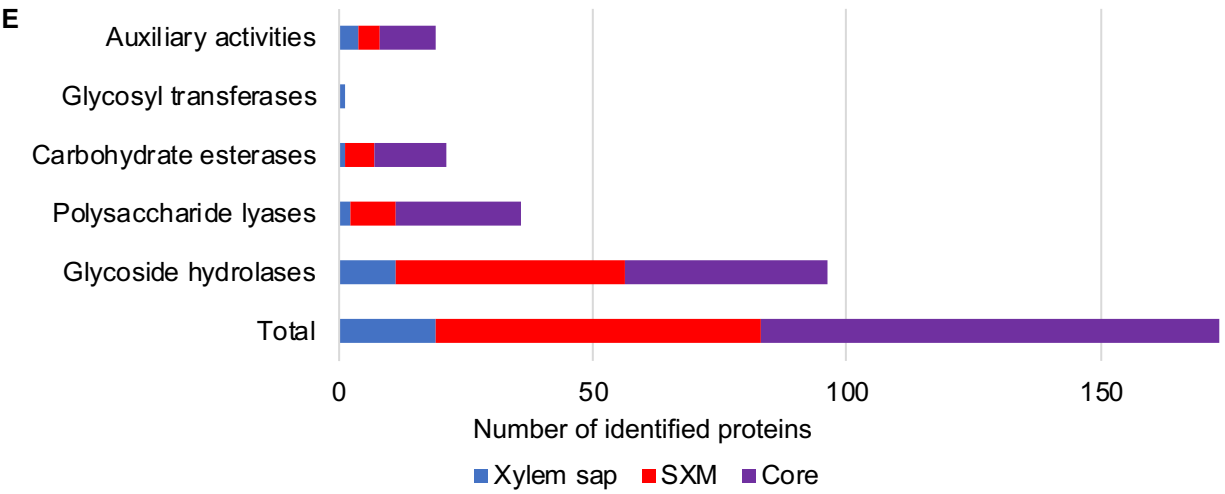
E
Auxiliary activities
Glycosyl transferases
Carbohydrate esterases
Polysaccharide lyases
Glycoside hydrolases
Total
0
50
100
150
Number of identified proteins
Xylem sap
SXM
Core

Figure 2

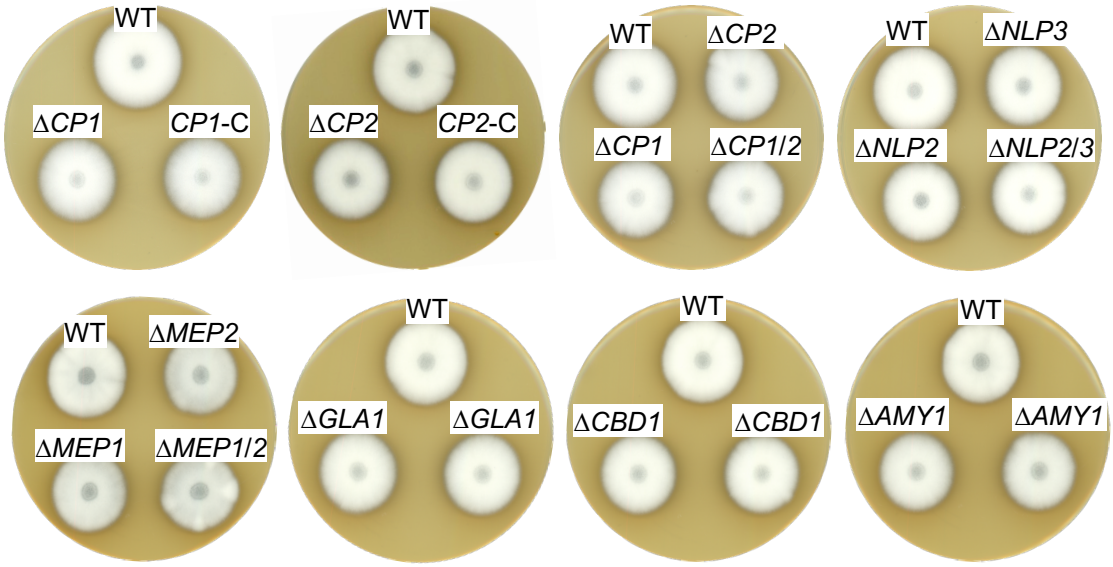
WT
ΔCP1
CP1-C
WT
ΔCP2
CP2-C
WT
ΔCP2
ΔCP1
ΔCP1/2
WT
ΔNLP3
ΔNLP2
ΔNLP2/3
WT
ΔMEP2
ΔMEP1
ΔMEP1/2
WT
ΔGLA1
ΔGLA1
WT
ΔCBD1
ΔCBD1
WT
ΔAMY1
ΔAMY1

Figure 3

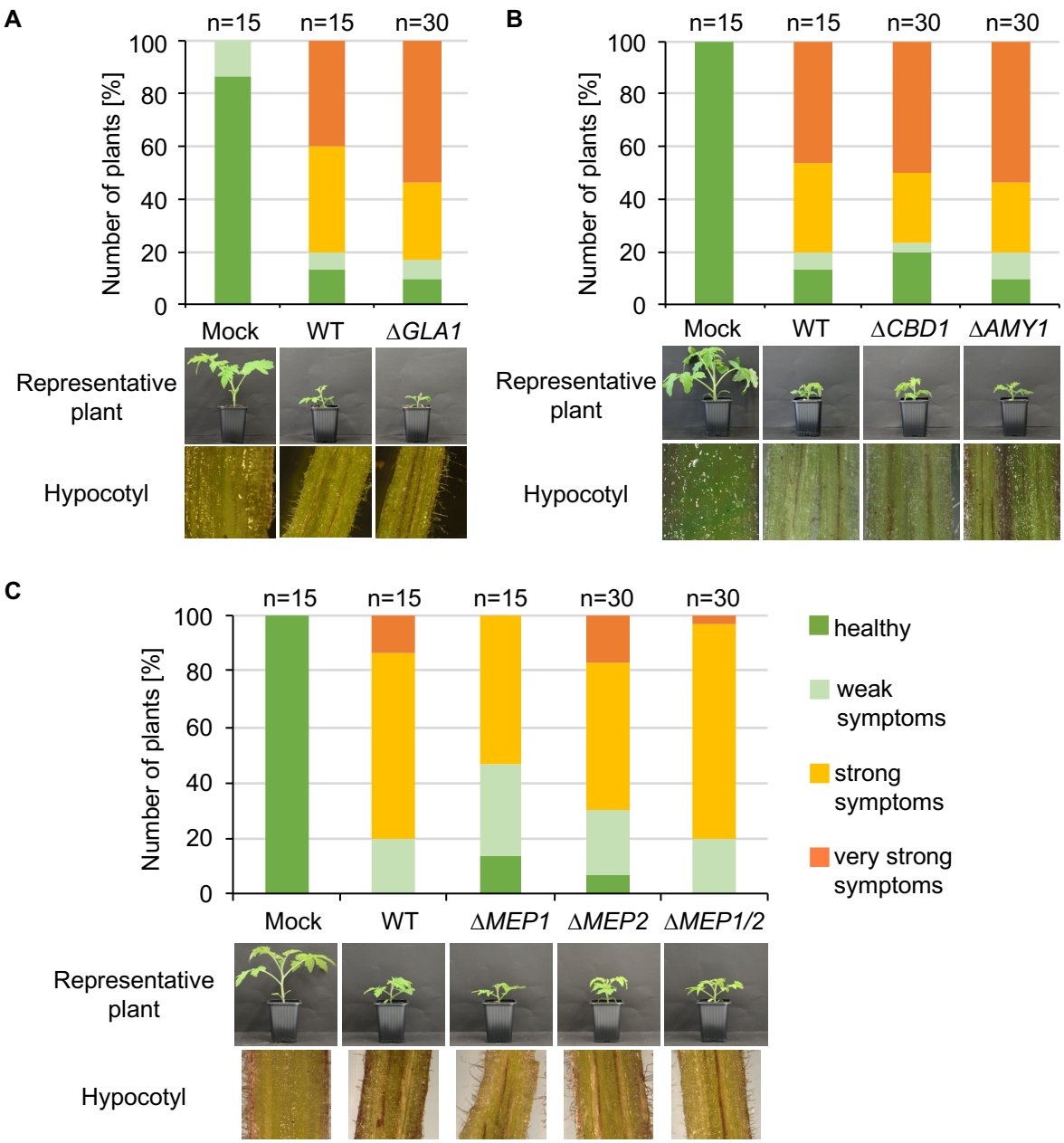
A
n=15
n=15
n=30
Number of plants [%]
100
80
60
40
20
0
Mock
WT
ΔGLA1
Representative plant
Hypocotyl
B
n=15
n=15
n=30
n=30
Number of plants [%]
Mock
WT
ΔCBD1
ΔAMY1
Representative plant
Hypocotyl
C
n=15
n=15
n=15
n=30
n=30
Number of plants [%]
Mock
WT
ΔMEP1
ΔMEP2
ΔMEP1/2
Representative plant
Hypocotyl
healthy
weak symptoms
strong symptoms
very strong symptoms

Figure 4

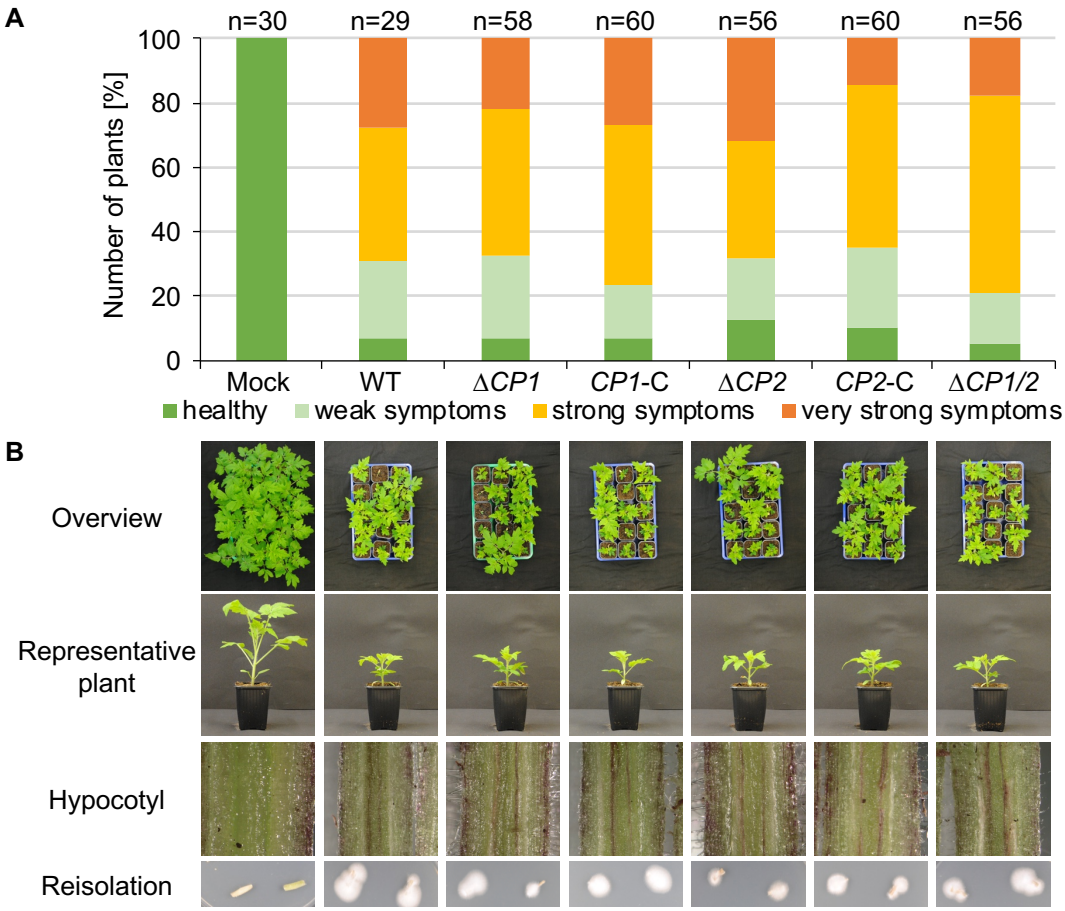
A
n=30
n=29
n=58
n=60
n=56
n=60
n=56
100
80
60
40
20
0
Number of plants [%]
Mock
WT
ΔCP1
CP1-C
ΔCP2
CP2-C
ΔCP1/2
healthy
weak symptoms
strong symptoms
very strong symptoms
B
Overview
Representative plant
Hypocotyl
Reisolation

Figure 5

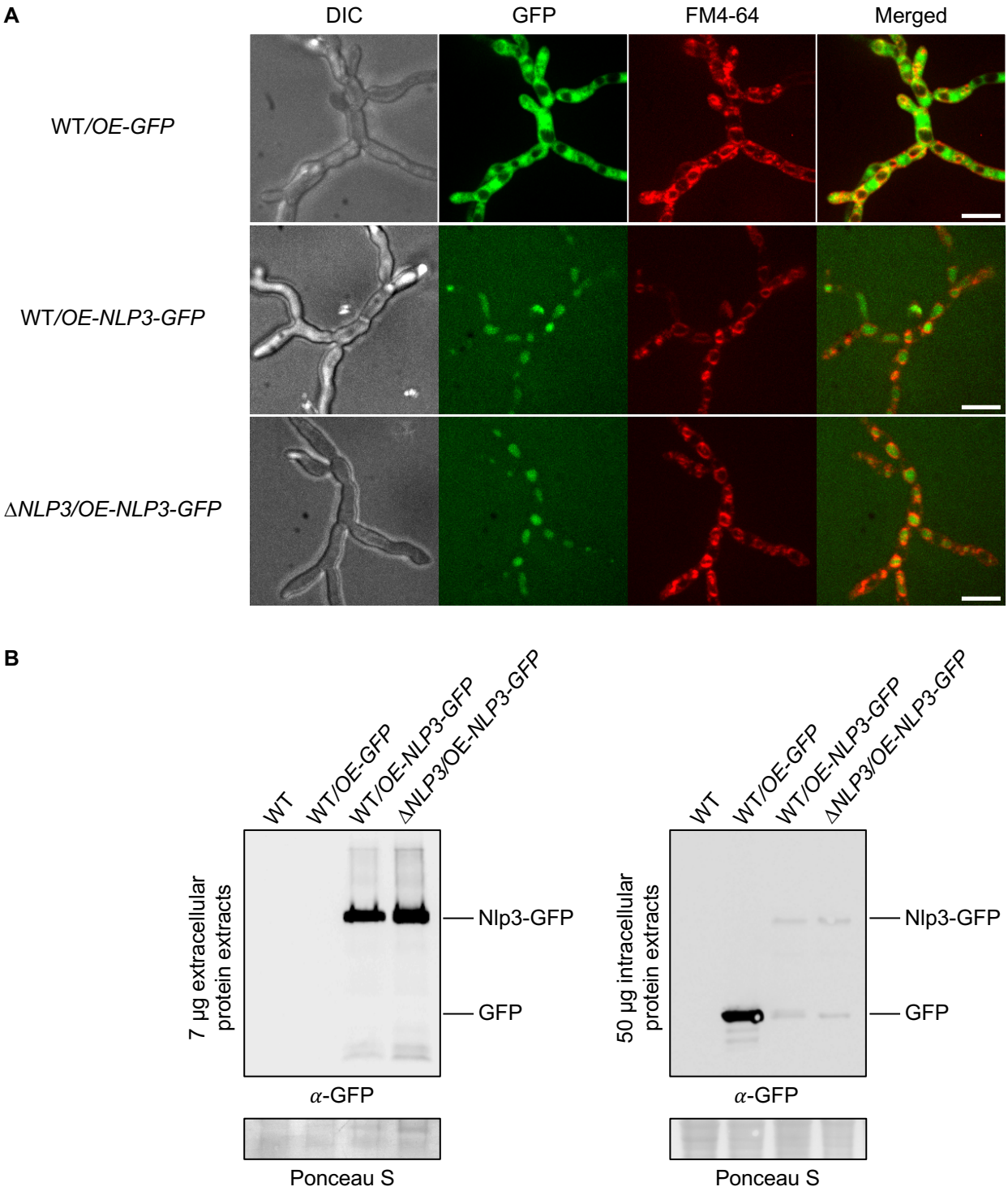
A
DIC
GFP
FM4-64
Merged
WT/OE-GFP
WT/OE-NLP3-GFP
ΔNLP3/OE-NLP3-GFP
B
WT
WT/OE-GFP
WT/OE-NLP3-GFP
ΔNLP3/OE-NLP3-GFP
7 µg extracellular protein extracts
Nlp3-GFP
GFP
α-GFP
Ponceau S
50 µg intracellular protein extracts
Nlp3-GFP
GFP
α-GFP
Ponceau S

Figure 6

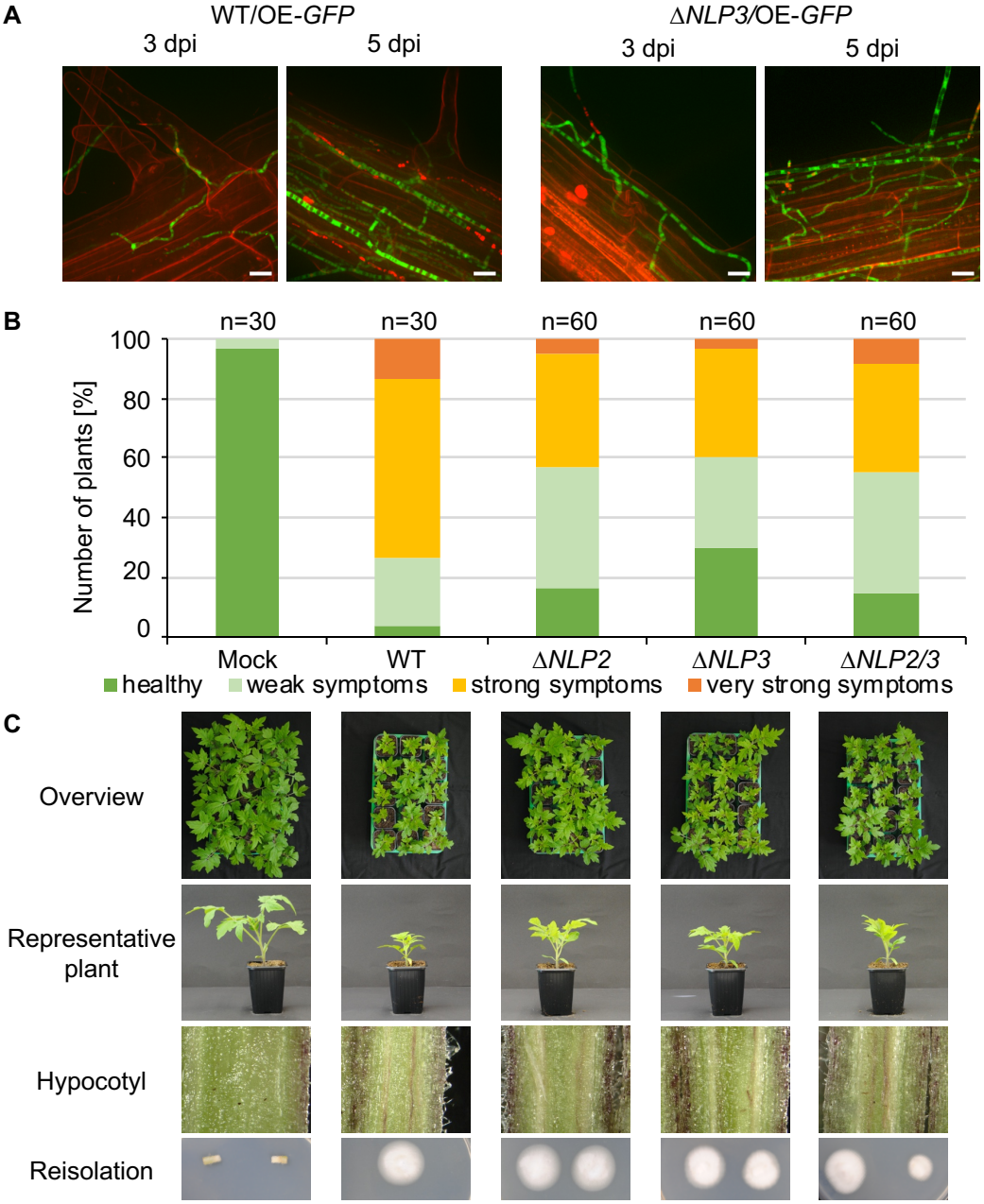
A
WT/OE-GFP
3 dpi
5 dpi
ΔNLP3/OE-GFP
3 dpi
5 dpi
B
n=30
n=30
n=60
n=60
n=60
100
80
60
40
20
0
Number of plants [%]
Mock
WT
ΔNLP2
ΔNLP3
ΔNLP2/3
healthy
weak symptoms
strong symptoms
very strong symptoms
C
Overview
Representative plant
Hypocotyl
Reisolation

Figure 7